Research Article | Vol. 30, No. 22 / 24 Oct 2022 / Optics Express 40779
Optics EXPRESS

Analytical Lah-Laguerre optical formalism for perturbative chromatic dispersion

DIMITAR POPMINTCHEV,[1,5] SIYANG WANG,[2] XIAOSHI ZHANG,[2,3] VENTZISLAV STOEV,[4] AND TENIO POPMINTCHEV[1,2,6]

[1]*Photonics Institute, TU Wien, Vienna A-1040, Austria*
[2]*University of California San Diego, Physics Department, and Center for Advanced Nanoscience, La Jolla, CA 92093, USA*
[3]*Aerospace Information Research Institute, Chinese Academy of Sciences, Beijing 100094, China*
[4]*LEMA Photonics Ltd, Veliko Tarnovo 5000, Bulgaria*
[5]*dimitar.popmintchev@gmail.com*
[6]*tenio.popmintchev@physics.ucsd.edu*

Abstract: We present a generalized perturbative analytical formalism for evaluation and optimization of the chromatic dispersion of complex ultrafast optical systems. Notably, we identify polynomial and recursive relations associated with the chromatic dispersion orders that are identical to the Lah and Laguerre transforms. We explicitly outline the first ten dispersion terms and dispersion slope parameters and visualize the significance of the chromatic dispersion orders for several advanced ultrafast optical and photonic systems consisting of various optical materials and nanostructures, grating and prism-pair compressors, and hollow-core photonic anti-resonant fibers. The derived simple hypergeometric transforms are applicable for evaluation of infinitely high orders for any type of frequency-dependent phase and can facilitate the optimization of complex optical systems with controlled dispersion balance at the single-cycle waveform extreme.

1. Introduction

Often assumed negligible, the high chromatic dispersion orders are commonly ignored in complex ultrafast optical system designs and analyses. In the present study, we revisit this longstanding, classical phenomenon, dating back to the research of Pierre Laplace and George Airy on the dispersion of water waves, and of Ernst Abbe on the dispersion in optical systems. However, we approach these analyses with a new emphasis on obtaining generalized closed-form expressions for the chromatic dispersion orders, and further unveiling their significance in the propagation dynamics of ultrashort single-cycle laser pulses for cutting-edge dispersion control. Considering that the accuracy of the evaluated dispersion orders is linked to the precision with which the phase, the optical path, or the refractive index are specified, and vice versa, this formalism can also facilitate more precise interferometric measurements of the refractive index and aid the design of novel optical materials, nanostructures, and optical systems based on desired dispersion. Furthermore, from a practical point of view, the evaluation speed of the simple hypergeometric series can be competitive even against algorithms such as the fast Fourier transform (FFT).

The chromatic dispersion phenomenon has worked both in favor of and against some of the most significant innovations in optics and photonics in the past decades. The group delay dispersion (*GDD*) and the higher orders of dispersion have been a major hindrance to the expansion of the fiber-based telecommunications. With the ever-growing need to increase the bit-rate-length transfer product through dispersion-optimized hair-thin fibers, the technology has been pushed to its limits. On one hand, pulsed signals are desired for information transfer. These pulses, on the other hand, are expected to retain their structure to the extent that the receiver can decode the data. Thus, the use of long narrow-band pulses at the zero *GDD* dispersion wavelength has been a compromise [1–5], considering that even a lengthy sub-picosecond, narrow-band pulse

#457139 https://doi.org/10.1364/OE.457139
Journal © 2022 Received 1 Mar 2022; revised 10 Jun 2022; accepted 10 Jun 2022; published 20 Oct 2022

Optics EXPRESS

may spread beyond recognition when propagating tens of kilometers. At present, the dispersion can be manipulated through sections of dispersion-shifted fibers, Bragg gratings, etc. However, counter-intuitively, operating away from the zero-dispersion is often advantageous for increased data transmission through multiple channels (wavelength division multiplexing), in which some residual dispersion is required by design to avoid signal distortions [6]. The performance of such frameworks can be enhanced through the precise calculation and control of the high orders of dispersion in the next-generation platforms.

In another field of optics and similarly to the radar ranging systems, the chirp pulse amplification technique – in which a pulse is first stretched in time to prevent optical damage, then amplified, and lastly compressed to femtosecond time scales – has opened the gateways to the development of immensely high-average power and high-peak power laser systems at high pulse repetition rates (kHz to MHz) [7–9]. At the same time, achieving transform-limited ultrashort pulse durations requires a nearly impossible balance of the chromatic dispersion acquired in the stretcher and the subsequent laser amplification stages in which the pulses accumulate a linear and nonlinear phase passing through lengthy sections of various materials. Whereas groove-matched or mismatched gratings or prism-based stretchers and compressors are suitable for compensation of the low chromatic dispersion orders, the adequate balance of the higher orders of dispersion is not always possible due to the different rates of linear or nonlinear phase accumulation [10,11]. In such scenarios, it is beneficial first to use advanced multilayered thin-film structures to passively mitigate the dispersion imbalance further, followed by additional active compensation of some of the remaining very high orders of dispersion [12–14]. However, generating near transform-limited laser pulses requires new apparatus and high-performance algorithms.

To address such challenges, our analyses begin with a detailed description and derivation of analytical closed-form dispersion expressions which, in the second part of the paper, are utilized to assess ultrahigh chromatic dispersion orders of various conventional ultrafast optical systems.

2. Analytical Lah-Laguerre optical formalism for chromatic dispersion

We start from first principles to craft an intuitive and comprehensive model of the perturbative chromatic dispersion. Any well-behaved wavepacket depicting a broadband laser pulse $E(\omega|\lambda) = |E|exp(-i\varphi(\omega|\lambda))$ in a dispersive medium, can be represented as a sum of sinusoidal wavelets traveling at different phase velocities that are frequency-dependant. The propagation of such a wave in a dispersive system is a linear and causal phenomenon that distorts the amplitude and the phase of the pulse in the temporal domain. First, we consider the laser intensities for which the interactions are linear. The dispersion relation for the phase is:

$$\varphi(\omega|\lambda) = k(\omega)z = \frac{\omega}{c}n(\omega)z = \frac{2\pi}{\lambda}n(\lambda)z = \frac{\omega}{c}OP(\omega) = \frac{2\pi}{\lambda}OP(\lambda) = \omega\tau(\omega) = \frac{2\pi}{\tau_0}\tau(\omega) \tag{1}$$

where $OP(\omega|\lambda)$ is the optical path, $n(\omega|\lambda)$ is the refractive index of the medium, $\tau(\omega|\lambda)$ is the corresponding temporal interval, and τ_0 is the single-cycle pulse duration for a wavelet with a wavelength λ. In such a picture, the spectral content of the signal does not change but rather rearranges temporally over a certain band around an average frequency ω_0. Historically, the dispersion orders have been defined in the frequency space through the Taylor expansion of the phase $\varphi(\omega|\lambda)$, or the wavevector $k(\omega|\lambda)$ around the pulse intensity-averaged frequency or the carrier frequency at the pulse peak [15]:

$$\begin{aligned}\varphi(\omega) &= \varphi\ |_{\omega_0} + \left.\frac{\partial\varphi}{\partial\omega}\right|_{\omega_0}(\omega-\omega_0) + \frac{1}{2}\left.\frac{\partial^2\varphi}{\partial\omega^2}\right|_{\omega_0}(\omega-\omega_0)^2 + \ldots + \frac{1}{p!}\left.\frac{\partial^p\varphi}{\partial\omega^p}\right|_{\omega_0}(\omega-\omega_0)^p + \ldots = \\ &= \varphi\ |_{\omega_0} + \tau_g\ |_{\omega_0}(\omega-\omega_0) + \frac{1}{2}GDD(\omega-\omega_0)^2 + \ldots + \frac{1}{p!}POD(\omega-\omega_0)^p + R_p\end{aligned} \tag{2}$$

Such a representation is convenient as it requires knowledge only of a small number of spectral derivatives at a single point. The first derivative $\left.\frac{\partial\varphi}{\partial\omega}\right|_{\omega_0} = \tau_g$ corresponds to the group delay

Optics EXPRESS

(*GD*), which results in a temporal lag of the pulse envelope. The presence of higher orders causes distortions in the temporal pulse shape. The second term $\frac{\partial^2\varphi}{\partial\omega^2}\Big|_{\omega_0} = \frac{\partial}{\partial\omega}\tau_g(\omega)\Big|_{\omega_0}$ corresponds to the group delay dispersion (*GDD*), and in general, $\frac{\partial^p\varphi}{\partial\omega^p}\Big|_{\omega_0} = \frac{\partial^{p-1}}{\partial\omega^{p-1}}\tau_g(\omega)\Big|_{\omega_0}$ is the p^{th} order dispersion (*POD*). Finally, $R_p = max_{\omega\le\xi\le\omega_0}\frac{\partial^{p+1}\varphi(\xi)}{\partial\xi^{p+1}}\frac{(\omega-\omega_0)^{p+1}}{(p+1)!}$ is the Lagrange error after the first p terms. This description requires knowledge of the particular $\tau_g(\omega)$ and can be used to derive recursive expressions for functions with repetitive or sequential derivatives [16]. Inverse chain rules need to be considered to estimate the chromatic dispersion when $\omega(\tau_g)$ can be easily specified, as in the case of the chromatic dispersion in extreme high order harmonic generation [17–19]. The perturbative representation for the chromatic dispersion is ideal for optimization problems in which the dispersion originating from several sources and at variable levels of the pulse intensity must be precisely balanced, e.g., in complex laser chirped pulse amplification systems, as opposed to situations where the effect on the pulse propagation caused by uniform dispersive systems is of interest, e.g., in waveguiding photonic structures in which such perturbative approximations can be avoided [20–22].

In a similar fashion, the wavevector $k(\omega|\lambda)$ can be expanded in a Taylor series [15]:

$$\begin{aligned} k(\omega) =& k|_{\omega_0} + \frac{\partial k}{\partial\omega}\Big|_{\omega_0}(\omega-\omega_0) + \frac{1}{2}\frac{\partial^2 k}{\partial\omega^2}\Big|_{\omega_0}(\omega-\omega_0)^2 + \cdots + \frac{1}{p!}\frac{\partial^p k}{\partial\omega^p}\Big|_{\omega_0}(\omega-\omega_0)^p + \cdots = \\ &= k_0 + v_{gr}^{-1}(\omega-\omega_0) + \frac{1}{2}GDD(\omega-\omega_0)^2 + \cdots + \frac{1}{p!}POD(\omega-\omega_0)^p + R_p \end{aligned} \tag{3}$$

Again, the lowest term $\frac{\partial k}{\partial\omega}\Big|_{\omega_0} = \frac{1}{v_g} = \frac{\tau_g}{z}$ represents the inverse group velocity, whereas the second term $\frac{\partial^2 k}{\partial\omega^2}\Big|_{\omega_0} = \frac{\partial}{\partial\omega}v_{gr}^{-1}\Big|_{\omega_0}$ represents the *GDD*. In general, $\frac{\partial^p k}{\partial\omega^p}\Big|_{\omega_0} = \frac{\partial^{p-1}}{\partial\omega^{p-1}}v_{gr}^{-1}\Big|_{\omega_0}$ is the p^{th} order dispersion (*POD*), which may be significant in ultrashort pulse propagation. When pulses have a substantial spectral bandwidth, it is necessary to consider many of the high orders in the Taylor expansion. Recursive relations of the dispersion orders and their effects on the pulse broadening for specific systems, such as optical fibers and waveguides, have previously been investigated [23,24].

In the following paragraphs, we derive a closed-form, general, Lah-Laguerre optical formalism (LLOF) for the dispersion orders of an optical system described by a known phase $\varphi(\omega|\lambda)$, a refractive index $n(\omega|\lambda)$, or an optical path $OP(\omega|\lambda)$. The chromatic dispersion orders can be easily evaluated in the frequency domain by obtaining the successive derivatives of the wavevector $k(\omega)$ or the phase $\varphi(\omega)$. The first ten terms are specified in Appendix A and C. In general:

$$\frac{\partial^p}{\partial\omega^p}k(\omega) = \frac{1}{c}\left(p\frac{\partial^{p-1}}{\partial\omega^{p-1}}n(\omega) + \omega\frac{\partial^p}{\partial\omega^p}n(\omega)\right) = \frac{\omega^{1-p}}{c}\sum_{m=0}^{p}\mathcal{V}(p,m)\omega^m\frac{\partial^m}{\partial\omega^m}n(\omega) \tag{4}$$

$$\frac{\partial^p}{\partial\omega^p}\varphi(\omega) = \frac{1}{c}\left(p\frac{\partial^{p-1}}{\partial\omega^{p-1}}OP(\omega) + \omega\frac{\partial^p}{\partial\omega^p}OP(\omega)\right) = \frac{\omega^{1-p}}{c}\sum_{m=0}^{p}\mathcal{V}(p,m)\omega^m\frac{\partial^m}{\partial\omega^m}OP(\omega) \tag{5}$$

where $p = 1, 2, 3\ldots$ are integral numbers. The matrix coefficients $\mathcal{V}(p,m) = p\delta_{p-1,m} + \delta_{p,m}$ up to the tenth order, $p\le10$, are listed in Table 1, Appendix A. The Kronecker delta function δ takes values $\delta_{p,m} = 1$ for $p = m$, and 0 otherwise. The inverse transforms can be expressed as: $\omega^p\frac{\partial^p}{\partial\omega^p}f(\omega) = (-1)^p\frac{c}{\omega}\sum_{m=0}^{p}\mathcal{E}(p,m)\omega^m\frac{\partial^m}{\partial\omega^m}\left(\frac{\omega}{c}f(\omega)\right)$, with f representing the refractive index $n(\omega)$ or the optical path $OP(\omega)$. The matrix coefficients $\mathcal{E}(p,m) = (-1)^m\frac{p!}{m!}$ are listed in Table 6, Appendix E. We evaluate consecutively the frequency and wavelength derivatives of $n(\omega|\lambda)$ or $OP(\omega|\lambda)$ as a function of the wavelength and the frequency. Despite the complexity, the

Optics EXPRESS

derivatives interestingly reduce to polynomials of the p^{th} order in λ or ω, which will further enable a closed-form expression formulation of the dispersion orders:

$$\frac{\partial^p}{\partial\omega^p}n(\omega) \;= (-1)^p\left(\frac{\lambda}{2\pi c}\right)^p \sum_{m=0}^{p} \mathcal{A}(p,m)\;\lambda^m \frac{\partial^m}{\partial\lambda^m}n(\lambda) \tag{6}$$

The spectral derivatives $\frac{d\omega}{d\lambda} = -\frac{\omega^2}{2\pi c}$ and $\frac{d\lambda}{d\omega} = -\frac{\lambda^2}{2\pi c}$ have the same functional form, and thus:

$$\frac{\partial^p}{\partial\lambda^p}n(\lambda) \;= (-1)^p\left(\frac{\omega}{2\pi c}\right)^p \sum_{m=0}^{p} \mathcal{A}(p,m)\;\omega^m \frac{\partial^m}{\partial\omega^m}n(\omega) \tag{7}$$

where $p = 0, 1, 2, 3, \ldots$ are integral numbers and the matrix $\mathcal{A}(p,m)$ is specified as: $\mathcal{A}(p,m) = \frac{p!}{(p-m)!m!}\frac{(p-1)!}{(m-1)!} = C(p,m)\frac{(p-1)!}{(m-1)!} = C(p{-}1,p{-}m)\frac{p!}{m!}$, with binomial coefficients $C(p,m) = \binom{p}{m} = \frac{p!}{(p-m)!m!}$. The matrix elements $\mathcal{A}(p,m)$ up to the tenth order are listed in Table 2, Appendix B. At $m = 0$, $\mathcal{A}(p,0) = 0$ for $p{\geq}1$, and $\mathcal{A}(0,0) = 1$. For reference, all derivatives up to the tenth order are specified in Appendix B.

In particular, we note that the matrix elements $\mathcal{A}(p,m)$ represent, amongst other known sub-series, the values of the Lah numbers [25–27]. In this context, the transformation of the derivatives from the frequency to the wavelength space, and vice versa, of any differentiable function can be intuitively viewed as a representation of a Lah transform. The forward $\mathcal{L}(x)$ and inverse $\mathcal{L}^{-1}(u)$ Lah transforms can be expressed as [28,29]:

$$u_p = \mathcal{L}(x) = (-1)^p \sum_{m=0}^{p} \mathcal{A}(p,m)\;x_m;\; x_p = \mathcal{L}^{-1}(u) = (-1)^p \sum_{m=0}^{p} \mathcal{A}(p,m)\;u_m \tag{8}$$

The polynomial sums in Eqs. (6)–(8), and Eqs. (10)–(14) form sequential polynomials $G_p^{(\alpha)}(x)$ for $\alpha = -1$. The corresponding generating function can be expressed as:

$$G_p^{(\alpha)}(x) = x^{-\alpha}\frac{d^p}{dx^p}\left(x^{p+\alpha}f(x)\right) = \sum_{m=0}^{p} C(p+\alpha, p-m)\frac{p!}{m!}x^m f^{(m)}(x) \tag{9}$$

where $f(x) \equiv G_0^{(\alpha)}$ is a smooth p-times-differentiable function, representing here either the refractive index n, the optical path OP, or the phase φ, and $f^{(m)}(x)$ is the m^{th} derivative of $f(x)$. Several physical properties of these generalized polynomials are examined in the next section. Similarly, we can write the Lah transforms for the optical path derivatives:

$$\frac{\partial^p}{\partial\omega^p}OP(\omega) = (-1)^p\left(\frac{\lambda}{2\pi c}\right)^p \sum_{m=0}^{p} \mathcal{A}(p,m)\;\lambda^m \frac{\partial^m}{\partial\lambda^m}OP(\lambda) \tag{10}$$

$$\frac{\partial^p}{\partial\lambda^p}OP(\lambda) = (-1)^p\left(\frac{\omega}{2\pi c}\right)^p \sum_{m=0}^{p} \mathcal{A}(p,m)\;\omega^m \frac{\partial^m}{\partial\omega^m}OP(\omega) \tag{11}$$

For completeness, we also include the Lah transforms in terms of the wavelength for the chain sequence $\frac{\partial^{p+1}}{\partial\omega^{p+1}}\varphi(\omega) = \left(-\frac{\lambda^2}{2\pi c}\right)\frac{\partial}{\partial\lambda}\left(\frac{\partial^p}{\partial\omega^p}\varphi(\omega)\right)$, which for numerical purposes can be recast more

Optics EXPRESS

conveniently as:

$$POD(\varphi) = \frac{\partial^p}{\partial\omega^p}\varphi(\omega) = (-1)^p\left(\frac{\lambda}{2\pi c}\right)^p \sum_{m=0}^{p} \mathcal{A}(p,m)\ \lambda^m \frac{\partial^m}{\partial\lambda^m}\varphi(\lambda) \tag{12}$$

$$\frac{\partial^p}{\partial\lambda^p}\varphi(\lambda) = (-1)^p\left(\frac{\omega}{2\pi c}\right)^p \sum_{m=0}^{p} \mathcal{A}(p,m)\ \omega^m \frac{\partial^m}{\partial\omega^m}\varphi(\omega) \tag{13}$$

From a practical point of view, when the *GDD* data is experimentally or numerically accessible in the wavelength space, the dispersion orders can be expressed as:

$$\frac{\partial^{p+2}}{\partial\omega^{p+2}}\varphi(\omega) = \frac{\partial^p}{\partial\omega^p}GDD = (-1)^p\left(\frac{\lambda}{2\pi c}\right)^p \sum_{m=0}^{p} \mathcal{A}(p,m)\ \lambda^m \frac{\partial^m}{\partial\lambda^m}GDD(\lambda) \tag{14}$$

By substituting the frequency derivatives from Eqs. (6) and (10) into the frequency dispersion relations Eqs. (4) and (5), we obtain further simplified closed-form expressions. The *POD* dispersion orders are reduced to polynomials of p^{th} order in λ. Accordingly, we arrive at another key expression for the p^{th} order chromatic dispersion:

$$POD(n) = \frac{\partial^p}{\partial\omega^p}k(\omega) = (-1)^p\frac{1}{c}\left(\frac{\lambda}{2\pi c}\right)^{p-1} \sum_{m=0}^{p} \mathcal{B}(p,m)\ \lambda^m \frac{\partial^m}{\partial\lambda^m}n(\lambda) \tag{15}$$

where $p = 0, 1, 2, 3, 4, \ldots$ are integral numbers. The matrix elements $\mathcal{B}(p,m) = \frac{p!}{(p-m)!m!}\frac{(p-2)!}{(m-2)!}$ $= \mathcal{A}(p,m)\frac{m-1}{p-1} = C(p,m)\frac{(p-2)!}{(m-2)!} = C(p{-}2,p{-}m)\frac{p!}{m!}$, up to the tenth order are tabulated in Table 3, Appendix C. At $m = 0$ or 1, $\mathcal{B}(p,[0,\ 1]) = 0$ for $p{\geq}2$, however, $\mathcal{B}(0,0) = 1$, $\mathcal{B}(1,0) = -1$, and $\mathcal{B}(1,1) = 1$. For reference, the *POD* chromatic dispersion expressions are explicitly outlined in Appendix C. Thus, the Lah-Laguerre optical formalism facilitates an infinite extension of the well-known low orders. Similarly, when a system is described by its optical path, the main expression for the p^{th} order chromatic dispersion reduces to:

$$POD(OP) = \frac{\partial^p}{\partial\omega^p}\varphi(\omega) = (-1)^p\frac{1}{c}\left(\frac{\lambda}{2\pi c}\right)^{p-1} \sum_{m=0}^{p} \mathcal{B}(p,m)\ \lambda^m \frac{\partial^m}{\partial\lambda^m}OP(\lambda) \tag{16}$$

Importantly, the matrix elements $\mathcal{B}(p,m) = \mathcal{A}(p,m)\frac{m-1}{p-1}$, denote the unsigned coefficients presented as a triangular or square array $i!\left[C(i{\pm}2,i{-}j)\frac{1}{j!}\right]$ for the generalized orthogonal Laguerre polynomials $L_i^{(\alpha)}(x)$ for $\alpha = -2$, or $\alpha = 2$ with shifted indices. The matrix elements $\mathcal{D}(p,m) = \mathcal{A}(p,m)\frac{p}{m}$ in Eq. (28) represent the unsigned coefficients for the orthogonal Laguerre polynomials $L_p^{(\alpha)}(x)$ for $\alpha = 0$ [27].

The generating function for the polynomial sums in Eqs. (15) and (16) can be expressed in terms of the already defined polynomial $G_p^{(\alpha)}(x)$ for $\alpha = -2$. Interestingly, the generating function for the polynomial sum in Eq. (28) can be expressed using the same $G_p^{(\alpha)}(x)$, albeit for $\alpha = 0$. For the Laguerre polynomials, the weight function is $f(x) = e^{-x}$. However, for the $G_p^{(\alpha)}(x)$ polynomials, the analogous weight function is trivially $f(x) \equiv G_0^{(\alpha)}(x) = e^{ln(f(x))}$ with $f(x)$ being a smooth p-times-differentiable expression representing the refractive index n or the optical path OP. The $G_p^{(\alpha)}(x)$ polynomials may not be orthogonal in general, however, they share several

Optics EXPRESS

similar relations with the Laguerre polynomials:

$$G_p^{(\alpha)}(x) = G_p^{(\alpha+1)}(x) - pG_{p-1}^{(\alpha+1)}(x) = p! \sum_{j=0}^{\beta} \binom{\beta}{j} \frac{(-1)^j}{(p-j)!} G_{p-j}^{(\alpha+\beta)}(x) \tag{17}$$

$$G_p^{(\alpha+1)}(x) = p! \sum_{j=0}^{p} \frac{1}{j!} G_j^{(\alpha)}(x)\ ;\ G_p^{(\alpha)}(x) = p! \sum_{j=0}^{p} \binom{\alpha+p-\beta}{p-j} \frac{1}{j!} G_j^{(\beta-j)}(x) \tag{18}$$

$$x^{p+\alpha} G_{p+1}^{(\alpha)}(x) = \frac{\partial}{\partial x}\left(x^{p+\alpha+1} G_p^{(\alpha)}(x)\right); G_{p+1}^{(\alpha)}(x) = x\frac{\partial}{\partial x} G_p^{(\alpha)}(x) + (p+\alpha+1)\, G_p^{(\alpha)}(x) \tag{19}$$

Using the above polynomials, the p^{th} order dispersion can now be expressed as:

$$POD\,(n|OP) = \frac{1}{c}(-1)^p \left(\frac{\lambda}{2\pi c}\right)^{p-1} G_p^{(-2)}(\lambda) = \frac{(-1)^p}{c}\left(\frac{\lambda}{2\pi c}\right)^{p-1}\left(G_p^{(-1)}(\lambda) - pG_{p-1}^{(-1)}(\lambda)\right) \tag{20}$$

Furthermore, taking into consideration Eq. (12), the p^{th} order dispersion $POD(\varphi)$ can be exclusively stated as:

$$POD(\varphi) = (-1)^p \left(\frac{\lambda}{2\pi c}\right)^p G_p^{(-1)}(\lambda)\ = (-1)^p \left(\frac{\lambda}{2\pi c}\right)^p \left(G_p^{(0)}(\lambda) - pG_{p-1}^{(0)}(\lambda)\right) \tag{21}$$

Accordingly, the group delay becomes $GD = -\frac{1}{c} G_1^{(-2)}(\lambda) = \frac{1}{c}\left(G_0^{(-1)}(\lambda) - G_1^{(-1)}(\lambda)\right)$.

In summary, the chromatic dispersion transformation from the frequency to the wavelength domain and vice versa is a generalized Laguerre type transform or a generalized Lah transform (LLOF). The forward $\mathcal{L}g^{(\alpha)}$ and inverse $\mathcal{L}g^{(\alpha)^{-1}}$ Laguerre transforms can be written as [26,29]:

$$u_p = \mathcal{L}g^{(\alpha)} = (-1)^p \sum_{m=0}^{p} \binom{p+\alpha}{p-m} \frac{p!}{m!}\, x_m;\ x_p = \mathcal{L}g^{(\alpha)^{-1}} = (-1)^p \sum_{m=0}^{p} \binom{p+\alpha}{p-m} \frac{p!}{m!}\, u_m \tag{22}$$

The Laguerre $\mathcal{L}g^{(\alpha)}$ and Lah $\mathcal{L}(x)$ transforms are interconnected: $\mathcal{L}g^{(\alpha)}(x) = P^{(\alpha)} P \mathcal{L}(x)$, where $P^{(\alpha)} = \binom{i+\alpha-j-1}{i-j} \frac{i!}{j!}$ is the permutation matrix [26]. Essentially, the Laguerre transform of order negative one, $\alpha = -1$, is equivalent to a Lah transform [30].

The refractive index $n(\lambda)$ and the optical path $OP(\lambda)$ are interchangeable in the closed-form chromatic dispersion equations, although the units must be suitably changed. The p^{th} order dispersion $POD(n)$ is measured in seconds to the power of p per unit of length $[s^p/m]$, whereas the units of the total dispersion $POD(\varphi|OP)$ are $[s^p]$. In fiber optics, a scaled group-delay dispersion is commonly used in units of $[s/nm]$ and $[s/nm/m]$: $SD(\varphi) = \frac{\partial \omega}{\partial \lambda} \frac{\partial \tau_g(\omega)}{\partial \omega}\Big|_{\omega_0} = -\frac{\omega_0^2}{2\pi c} GDD(\varphi)$ or $SD(n) = \frac{\partial \omega}{\partial \lambda} \frac{\partial}{\partial \omega}\left(\frac{1}{v_g}\right)\Big|_{\omega_0} = -\frac{\omega_0^2}{2\pi c} GDD(n)$. These entities effectively represent the temporal separation $\Delta\tau = SD(n) \cdot \ell \cdot \delta\lambda$ between two wavelength components spaced out by $\delta\lambda$ after a certain propagation length ℓ. Additionally, the higher derivatives $\frac{\partial^p}{\partial \lambda^p}\tau_g$ or $\frac{\partial^p}{\partial \lambda^p} v_{gr}^{-1}$ are often denoted as slopes of the dispersion parameters. Regarding the $p+1$ dispersion orders $\frac{\partial^p}{\partial \omega^p}\tau_g$ and $\frac{\partial^p}{\partial \omega^p} v_{gr}^{-1}$, the slope parameters can be formulated as:

$$\frac{\partial^p}{\partial \omega^p} v_{gr}^{-1}(\omega) = (-1)^p \left(\frac{\lambda}{2\pi c}\right)^p \sum_{m=0}^{p} \mathcal{A}(p,m)\, \lambda^m \frac{\partial^m}{\partial \lambda^m} v_{gr}^{-1}(\lambda) \tag{23}$$

$$\frac{\partial^p}{\partial \lambda^p} v_{gr}^{-1}(\lambda) = (-1)^p \left(\frac{\omega}{2\pi c}\right)^p \sum_{m=0}^{p} \mathcal{A}(p,m)\, \omega^m \frac{\partial^m}{\partial \omega^m} v_{gr}^{-1}(\omega) \tag{24}$$

With the help of Eq. (15), the latter equality can be articulated in the wavelength space as: $\lambda^p \frac{\partial^p}{\partial \lambda^p} v_{gr}^{-1}(\lambda) = -\frac{1}{c} \sum_{m=0}^{p} \sum_{k=0}^{m+1} (-1)^{p-m} \mathcal{A}(p,m) \mathcal{B}(m+1,k)\, \lambda^k \frac{\partial^k}{\partial \lambda^k} n(\lambda)$. After simplification or

Optics EXPRESS

by direct evaluation of the derivatives, we can obtain the closed-form expression for the slope parameters:

$$\frac{\partial^p v_{gr}^{-1}(\lambda)}{\partial\lambda^p} = -\frac{1}{c}\left((p-1)\frac{\partial^p}{\partial\lambda^p}n(\lambda) + \lambda\frac{\partial^{p+1}}{\partial\lambda^{p+1}}n(\lambda)\right) = -\frac{\lambda^{-p}}{c}\sum_{m=0}^{p+1}\mathcal{K}(p,m)\lambda^m\frac{\partial^m}{\partial\lambda^m}n(\lambda) \tag{25}$$

where $p = 1, 2, 3\ldots$ are integral numbers. The matrix coefficients $\mathcal{K}(p,m) = (p-1)\delta_{p,m} + \delta_{p+1,m}$, up to the tenth order are listed in Table 4, Appendix D. For reference, all closed-form expressions up to the tenth order are summarized in Appendix D. The inverse transform can be formulated as: $\lambda^p\frac{\partial^p}{\partial\lambda^p}n(\lambda) = (-1)^{p+1}c\sum_{m=0}^{p-1}\mathcal{K}(p,m)^{-1}\lambda^m\frac{\partial^m}{\partial\lambda^m}v_{gr}^{-1}(\lambda)$, where the inverse coefficients $\mathcal{K}(p,m)^{-1} = (-1)^{m-1}\frac{(p-2)!}{(m-1)!}$, $m \le p-1$ are equivalent to the matrix elements $\mathcal{E}(p-2, m-1)$ with shifted indices, as indicated in Table 7, Appendix E. Thus, a refined linear and nonlinear refractive index function $n(\lambda)$ can be extracted from known dispersion orders or a known phase.

Similar generalizations can be obtained when the dispersion is formulated in the wavelength space:

$$k(\lambda) = k|_{\lambda_0} + \left.\frac{\partial k}{\partial\lambda}\right|_{\lambda_0}(\lambda-\lambda_0) + \frac{1}{2}\left.\frac{\partial^2 k}{\partial\lambda^2}\right|_{\lambda_0}(\lambda-\lambda_0)^2 + \cdots + \frac{1}{p!}\left.\frac{\partial^p k}{\partial\lambda^p}\right|_{\lambda_0}(\lambda-\lambda_0)^p + R_p \tag{26}$$

$$\varphi(\lambda) = \varphi|_{\lambda_0} + \left.\frac{\partial\varphi}{\partial\lambda}\right|_{\lambda_0}(\lambda-\lambda_0) + \frac{1}{2}\left.\frac{\partial^2\varphi}{\partial\lambda^2}\right|_{\lambda_0}(\lambda-\lambda_0)^2 + \cdots + \frac{1}{p!}\left.\frac{\partial^p\varphi}{\partial\lambda^p}\right|_{\lambda_0}(\lambda-\lambda_0)^p + R_p \tag{27}$$

The derivatives of the wavevector k and the phase φ with respect to the wavelength, obtained from Eqs. (5) and (13) and expressed in terms of the frequency, or through a direct differentiation in terms of the wavelengths, are:

$$\frac{\partial^p}{\partial\lambda^p}\left(\frac{2\pi}{\lambda}f(\lambda)\right) = (-1)^p 2\pi\left(\frac{\omega}{2\pi c}\right)^{p+1}\sum_{m=0}^{p}\mathcal{D}(p,m)\omega^m\frac{\partial^m}{\partial\omega^m}f(\omega) \tag{28}$$

$$\frac{\partial^p}{\partial\lambda^p}\varphi(\lambda) = \frac{\partial^p}{\partial\lambda^p}\left(\frac{2\pi}{\lambda}f(\lambda)\right) = (-1)^p 2\pi\lambda^{-(p+1)}\sum_{m=0}^{p}\mathcal{E}(p,m)\lambda^m\frac{\partial^m}{\partial\lambda^m}f(\lambda) \tag{29}$$

where $p = 0, 1, 2, \ldots$ are integral numbers. The matrix coefficients $\mathcal{D}(p,m) = \frac{p!}{(p-m)!m!}\frac{p!}{m!} = \mathcal{A}(p,m)\frac{p}{m}$, and $\mathcal{E}(p,m) = (-1)^m\frac{p!}{m!}$ up to the tenth order are listed in Table 5, and Table 6, Appendix E. The analytical expressions are presented explicitly up to the tenth order in Appendix E. The derivatives $\frac{\partial^p}{\partial\omega^p}\varphi(\omega)$ and $\frac{\partial^p}{\partial\lambda^p}\varphi(\lambda)$ are related through Eqs. (12) and (13). The matrix elements $\mathcal{D}(p,m)$ represent the unsigned coefficients for the orthogonal Laguerre polynomials $L_p^{(\alpha)}(x)$ for $\alpha = 0$ and follow the Laguerre transform. The inverse transform of Eq. (29) can be stated as: $\lambda^p\frac{\partial^p}{\partial\lambda^p}f(\lambda) = \frac{\lambda}{2\pi}\sum_{m=0}^{p}\mathcal{V}(p,m)\lambda^m\frac{\partial^m}{\partial\lambda^m}\left(\frac{2\pi}{\lambda}f(\lambda)\right)$, where the coefficients $\mathcal{V}(p,m)$ are listed in Table 1, Appendix A. Hence, a refined linear and nonlinear refractive index or an optical path function can be extracted from known phase derivatives at a single point. Furthermore, by altering the properties of novel materials and optical systems, the dispersion can be optimized in reverse.

Regarding the accuracy of the perturbative expansion, while the Taylor series of the phase is expected to converge for most functions of interest $f(x)$, convergence is not guaranteed. Nevertheless, we can obtain a rough estimate for the radius of convergence of the phase in Eqs. (2)

Optics EXPRESS

and (3) from the limit:

$$R = \lim_{p\to\infty}\left|\frac{c_{p+1}}{c_p}\right| \sim \underbrace{\lim_{p\to\infty}\left(1+\frac{\lambda^{p+1}\frac{\partial^{p+1}}{\partial\lambda^{p+1}}f(\lambda)}{\sum_{m=0}^{p}\mathcal{B}(p,m)\,\lambda^m\frac{\partial^m}{\partial\lambda^m}f(\lambda)}\right)}_{\epsilon(\omega_0)}\left(\frac{\lambda}{2\pi c}\right)\Bigg|_{\omega_0} |\omega-\omega_0| < 1 \qquad (30)$$

As a rule of thumb, convergence could be expected for $\Delta\omega = |\omega-\omega_0| < \omega_0/\epsilon(\omega_0)$, i.e. $|\lambda| < \frac{\epsilon(\lambda_0)}{1+\epsilon(\lambda_0)}\lambda_0$ or $|\Delta\lambda| \sim \lambda_0$. The Taylor series usually converge to the actual function value as the number of the included orders increases. However, adding successive ultrahigh orders, even within the radius of convergence does not necessarily lead progressively towards a superior approximation in domains far from the expansion point. For example, the addition of all fifteen orders to the propagation of a single-cycle laser pulse with an extremely broad bandwidth centered at a wavelength of 4.0 μm, analyzed in the next section in Fig. 1(B), results in a worse approximation than obtained considering the first fourteen orders, contrary to the ultraviolet (UV) pulse propagation at a wavelength of 0.3 μm.

Finally, as the laser intensity increases, the laser-mater interactions become nonlinear. The refractive index can be expressed as $n(r,t,\lambda) \cong n_0(\lambda) + n_2(\lambda)I(r,t) + n_4(\lambda)I^2(r,t) + \ldots$, assuming an instantaneous nonlinear response and intensities $I(r,t)$ within the radius of convergence. Here, n_0 is the linear refractive index, all n_i ($i \geq 2$) represent the nonlinear refractive indices, and $I(r,t)$ is the pulse intensity. Now, the phase $\varphi = \frac{2\pi}{\lambda}n(r,t,\lambda)dz$ depends on the intensity and the polarization, and changes in space and time. This situation leads to numerous self-action effects, i.e., self-focusing, self-defocusing, self-phase modulation, temporal self-compression, solitons in space and time, etc. [3,15,31]. Although the presented chromatic dispersion relations discussed above remain unchanged, a series of approximations must be made in order to estimate the pulse shape distortions during propagation, which is beyond the scope of this study.

3. Chromatic dispersion in conventional ultrafast systems

As an illustration of the importance of the very high dispersion orders and demonstrating the simplicity and reduced computational load of the Lah-Laguerre optical formalism attained using the polynomial dispersion expressions, we describe several advanced areas of applications.

The derivatives of the phase, the refractive index, or the optical path length are required up to the highest order of the considered dispersion, and they need to be evaluated just once. We use analytical Sellmeier equations to determine the refractive index in cases involving material dispersion. The derivatives of the refractive index, the phase, or the optical path are obtained through symbolic evaluations. Numerically, this framework is highly efficient. For extremely high orders, the calculation speed can be increased by using recursive relations to determine the derivatives of the refractive index [5].

First, we consider the material dispersion of CaF_2, which is frequently encountered in broadband ultrafast laser applications. For this purpose, we use the analytical Sellmeier equation for the refractive index $n(\lambda)$ in the spectral region of 0.15 μm – 12 μm [32,33]. Although CaF_2 exhibits a small orientational birefringence at wavelengths less than 0.2 μm, the largest magnitude of the intrinsic birefringence is in the order of 10^{-6} [34], which is less than the accuracy of the measured index of refraction in that region. The first ten chromatic dispersion orders are shown in a bi-symmetric log plot [35] in Fig. 1(A). The high dispersion orders in the UV spectral domain exhibit extremely low values that increase in magnitude by $10^2 - 10^{10}$ times towards the mid-infrared (mid-IR). All odd orders are positive and result in a non-symmetrical pedestal pulse formation. Whereas the even orders undergo a sign change at the zero-crossing points, located approximately between 0.3 μm and 1.55 μm. In contrast, their effect in the time domain is a symmetric pulse broadening. As a rule of thumb, the dispersion effects on the

Optics EXPRESS

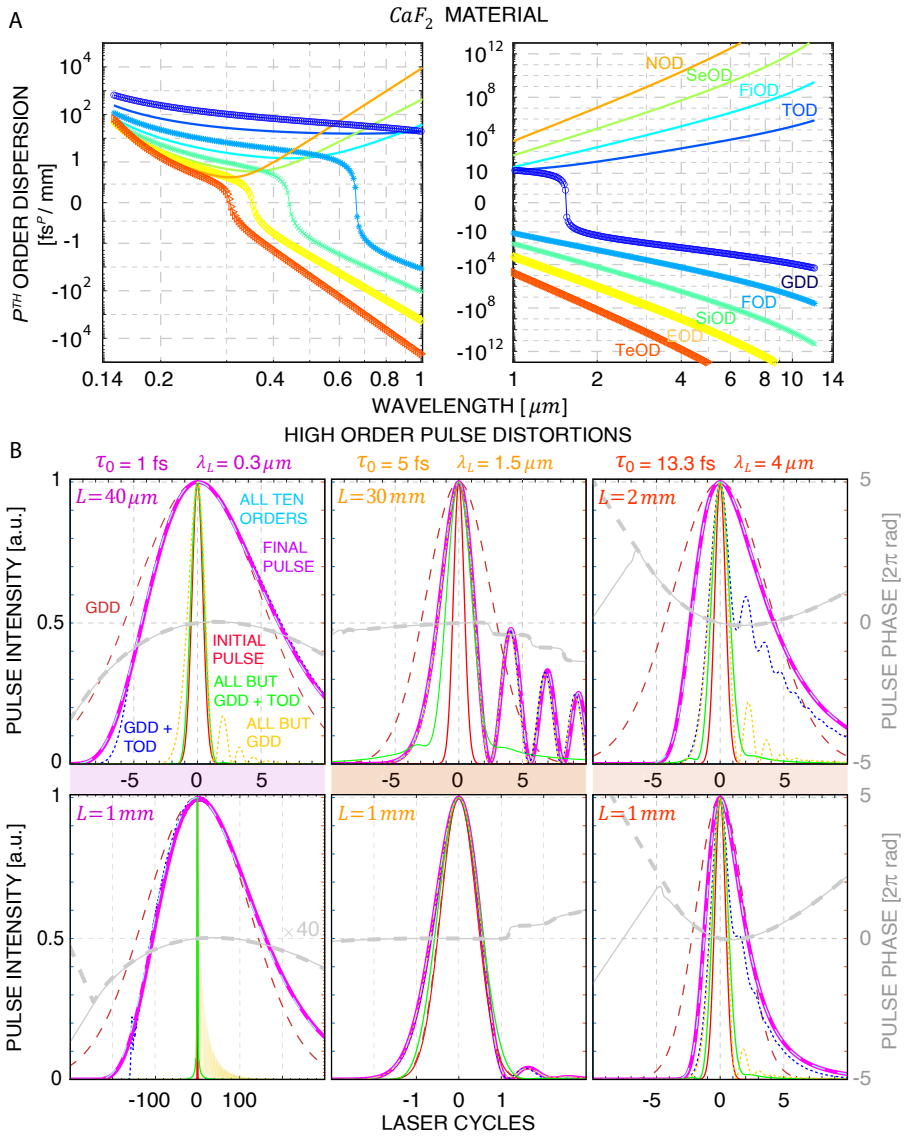

Fig. 1. Effect of ultrahigh dispersion orders on the temporal evolution of laser pulses at the single-cycle waveform extreme in the UV, near-IR, and mid-IR spectral regions. A) Material dispersion of p^{th} order up to the tenth order, $2 \leq p \leq 10$, for a CaF_2, indicating the zeros of the even orders and the significant increase in the magnitude of the dispersion orders towards the mid-IR wavelengths. B) (Top row) Evolution of single-cycle laser pulses versus time (in τ_0 cycles) in the UV, near-IR, and mid-IR regions at $\lambda_L = 0.3\ \mu m$, near the zero GDD at $\lambda_L = 1.5\ \mu m$, and $\lambda_L = 4\ \mu m$, respectively, after propagation through CaF_2 for the same accumulated phase of 4π, corresponding to thicknesses of $L = 40\ \mu m$, $L = 30\ mm$, and $L = 2\ mm$, respectively. (Bottom row) Comparison of the evolution of the single-cycle laser waveforms for an equal propagation length $L = 1\ mm$. The effects of the GDD and the combination of GDD and TOD are represented by the dashed burgundy and dotted blue curves, respectively. The effects of considering all orders up to the tenth order and only the high orders, specifically $3 \leq p \leq 10$ (all but GDD) and $4 \leq p \leq 10$ (all but GDD and TOD) are represented by the dashed cyan, orange and green curves, respectively. The final pulse broadening evaluated using the exact total phase is shown in purple. The temporal phase of the pulse $\phi(t)$ is depicted in dashed and solid gray, evaluated using only the first ten dispersion orders and exact calculations.

Optics EXPRESS

pulse broadening are substantial when $\frac{POD(\phi)}{\tau^p}$ is not negligible, where τ is the temporal pulse duration. The upper row of Fig. 1(B) shows a comparison of the pulse broadening for ultrashort, single-cycle, Gaussian pulses centered at UV, near-IR, and mid-IR wavelengths of $\lambda_L = 0.3\ \mu m$, $\lambda_L = 1.5\ \mu m$, and $\lambda_L = 4\ \mu m$ during linear propagation through a CaF_2 optical element with a thickness of $L = 40\ \mu m$, $L = 30\ mm$, and $L = 2\ mm$, respectively. The propagation lengths are chosen such that the accumulated relative phase of the pulses changes in the order of 4π radians in the time domain. We visualize the strength of the distortion effects associated with individual dispersion orders or a group of orders, in terms of the pulse duration and compare the pulse shapes to the exact pulse shape distorted by the accumulated total spectral phase $\varphi = \frac{2\pi}{\lambda} n(\lambda) z$. All temporal shapes $E(t) = |E| exp(-i\phi(t))$, where $\phi(t)$ denotes the temporal phase, are obtained through Fourier transforms of the pulse waveforms. Consideration of the first ten chromatic orders results in a near-perfect approximation of the dispersion effects compared to that achieved in the evaluation of the pulse shape using the exact total spectral phase φ. The single-cycle laser pulses have extremely broad spectral content and are considerably influenced also by the high orders of dispersion. In the UV spectral range, the high orders of dispersion have relatively low values per unit length, as shown in Fig. 1(A), and the main pulse broadening effect is dominated by the *GDD* and the third-order dispersion (*TOD*), which have the largest magnitude. The distortions associated with the high orders of dispersion are smaller but not negligible for large propagation distances. In contrast, in the mid-IR spectral region, the high dispersion orders are significantly more pronounced. This indicates that near-transform-limited few-cycle laser pulses can be realized more conveniently in practice in spectral regions with low values of the high orders, typically in the UV spectral region, by balancing fewer dispersion orders, mainly those associated with the *GDD* and the *TOD*. However, special precautions need to be taken for UV pulses to avoid propagation through any substantial amount of material, leading to the extremely fast pulse spreading. The bottom row of Fig. 1(B) illustrates the pulse broadening for the same propagation length $L = 1\ mm$, indicating the fast pulse broadening in the UV, dictated primarily by the *GDD* and the *TOD*. The same qualitative behavior with more pronounced effects is observed for the fused silica-based glasses, predominantly used in the fiber telecommunication. The significant pulse spread can be partially mitigated by operating near the zero *GDD* dispersion wavelength and using long picosecond narrow-bandwidth pulses. The *TOD* dominates the pulse spread in this scenario. However, the very high dispersion orders become significant at longer technologically relevant propagation scales. For single-cycle femtosecond pulses at $1.5\ \mu m$ (near the zero-dispersion *GDD* of CaF_2), an analogous picture involving a significant pulse modulation is observed, wherein the higher orders $p \geqslant 4$ contribute mostly to the broadening of the main pulse structure, which contains most of the energy, and to the formation of wings. This phenomenon indicates that to design dispersion-compensating systems for single-cycle near-IR and mid-IR pulses, novel advanced passive and active dispersion approaches must be used to balance and address the low- and high-order effects.

In general, the trend for the refractive index of materials with normal dispersion, far from the UV–extreme UV (EUV) absorption peaks, is smooth, corresponding to a monotonically decreasing functional form with an inflection point usually in the IR region for solids, the IR–far-IR region for gases, and the visible (VIS)–IR region for liquids, in which the zero *GDD* dispersion wavelength is located. Consequently, the odd-order derivatives of the refractive index are positive, and a step-like switching from positive to negative values is observed for the even-order derivatives. Gases at standard conditions exhibit mostly positive dispersion order values in the UV–VIS–IR region. For reference, data files and plots of the material dispersion of CaF_2, sapphire, fused silica, *BK7, BBO* (for the ordinary and extraordinary axes), water, liquid *Ar*, and several gases at standard conditions (air, *He*, *Ne*, *Ar*, *Kr*, *Xe*, H_2, O_2, and N_2), decomposed into the first ten orders using the Lah-Laguerre optical formalism, are available in Dataset 1, Ref. [36].

Optics EXPRESS

Subsequently, we consider the chromatic dispersion of a reflective grating compressor with a spectral phase $\varphi(\lambda) = \frac{\omega}{c} OP(\lambda)$ and a total optical path $OP(\lambda) = 2L\sqrt{1 - (m\sigma\lambda - sin(\vartheta))^2}$, where L is the grating separation, σ is the grating groove density, m is the diffraction order, and ϑ is the incident angle (Fig. 2(A)) [10,37]. Owing to the parameter space L and ϑ, a certain amount of GDD can be preserved when adjusting a desired order, albeit at the cost of the compressor throughput efficiency.

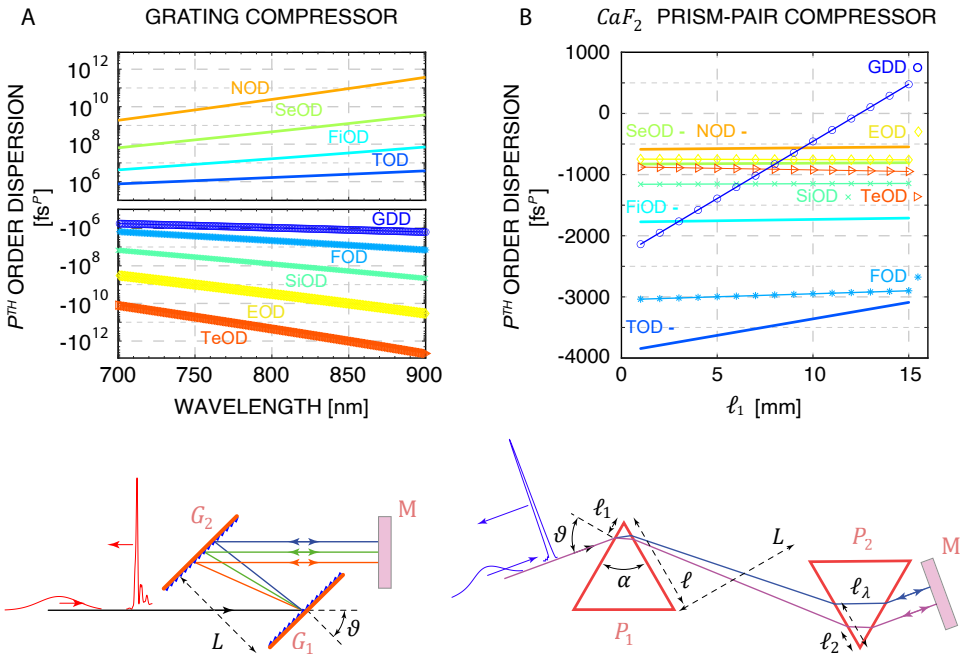

Fig. 2. High chromatic dispersion orders in ultrafast pulse compression systems in the UV and IR spectral regions. Top: Chromatic dispersion up to the tenth order, $2 \le p \le 10$, A) in a reflection-grating compressor in the near-IR around $\lambda_L = 0.8\ \mu m$, and B) in a prism-pair compressor in the UV spectral region around $\lambda_L = 0.4\ \mu m$, where CaF_2 has low values of the high dispersion orders (Fig. 1(A)). Bottom: Schematics of the considered designs, where G_i, P_i, and M denote gratings, prisms, and retroreflecting mirrors, respectively.

The first ten chromatic dispersion orders for a conventional ultrashort near-IR pulse compressor operating near $\lambda_L = 0.8\ \mu m$, are analyzed, as shown in Fig. 2(A), for $L = 30\ cm$, $\sigma = 1200\ lines/mm$, $m = 1$, and $\vartheta = 38^\circ$. For a case where blazed gratings may be considered, the highest diffraction efficiency is at $\lambda_L = 2sin(\delta_B)cos(\vartheta - \delta_B)/m\sigma$, with δ_B representing the blaze angle. As shown in Fig. 2(A), the high dispersion orders are significant – even a single fourth-order can distort a few-cycle laser pulse, rendering grating compressors incapable of realizing the fine compensation of the linear and the nonlinear phases of temporally and spectrally broadened pulses due to material dispersion. In general, the values of the high orders of dispersion of the compressor decrease towards the UV–EUV range, leaving the second and the third orders dominant. Although the GDD can be balanced, the residual high orders persist. A similar situation may be encountered in attosecond EUV pulse compression based on grating structures, where the phase of the EUV pulses may not be fully compensated due to the mismatch with the high dispersion orders.

In summary, the reflective-grating compressor phase shows monotonically increasing values, with even and odd optical-path derivatives exhibiting a negative and positive sign, respectively.

Optics EXPRESS

Transmission-grating compressors exhibit similar behavior with few minor differences. The incident angle can be designed to match the Littrow angle $\vartheta_L = asin(m\sigma\lambda/2)$, thereby achieving a higher transmission capacity and a lower angular sensitivity. By adding the dispersion contribution of the grating substrates, we can obtain the optical path of a transmission-grating compressor: $OP(\lambda) \cong 2L\sqrt{1-(m\sigma\lambda - sin(\vartheta))^2} + \frac{4\ell n^2}{\sqrt{n^2-sin^2\vartheta}}$, where ℓ and n denote the substrate thickness and the refractive index, respectively. These approximations correspond to a thin transmission grating with a grating equation at the glass-air interface, $-nsin(\vartheta_i) + n_0 sin(\vartheta_m) = -m\sigma\lambda$, where ϑ_i is the angle inside the substrate ($sin(\vartheta) = nsin(\vartheta_i)$), and ϑ_m represents the diffracted angles with $n_0 \cong 1$.

In state-of-the-art laser architectures in which dispersion balance is essential, phase-compensating compressors are often designed with matched or mismatched stretchers by introducing achromatic lenses, prisms, glass plates, grisms, and other optical elements inside the stretcher or the compressor [38–41]. These complex tuning designs cannot be easily implemented, necessitate individual and precise high-order dispersion calculations, and primarily suffer from the nonlinear phase accumulation that limits the energy and the peak power to relatively modest values. Additionally, chirped mirrors can be used to combat the low orders of dispersion. Typically, a linear or a curved *GDD* chirped mirror can be designed to introduce *GDD* and specific *TOD* and *FOD* with different slopes and curvatures to tune the *TOD* and the *FOD* of the grating-based stretchers and compressors in the chirped-pulse amplifiers [42]. The higher-order dispersion terms remain of great significance when a transform-limited single-cycle pulse duration must be ensured. In such circumstances, first, passive compensation is employed to eliminate the lower orders. Subsequently, active, adaptive compensation, such as spatial light modulators and acousto-optical programmable dispersive filters (e.g., Dazzler, Mazzler, etc.), is used to balance the remaining low and higher orders to a certain extent. An ordinary prism-pair compressor can also be employed to passively reduce a particular high order of dispersion while not affecting the *GDD* or other orders [43].

Next, we evaluate the chromatic dispersion orders of a prism-pair compressor for UV laser pulses in a model, considering the finite spectral bandwidth of an ultrashort pulse, including the material dispersion of the prisms [11,15,43,44]. In the schematic shown in Fig. 2(B), the optical path can be described as: $OP(\lambda) = 2\left(\ell_1 \frac{n^2 sin(\alpha)}{A(\lambda)} + \frac{L}{B(\lambda)} + \ell sin(\vartheta) + \ell_\lambda \frac{n^2 sin(\alpha) - A(\lambda) sin(\vartheta)}{D(\lambda)}\right)$, where $\ell_\lambda = \ell_2 + L\left(\frac{C(\lambda_m)}{B(\lambda_m)} - \frac{C(\lambda)}{B(\lambda)}\right) + \ell_1 nsin(\alpha)\left(\frac{1}{A(\lambda_m)} - \frac{1}{A(\lambda)}\right)$, $D(\lambda) = \sqrt{n^2 - sin^2(\vartheta)}$, $A(\lambda) = cos(\alpha)D(\lambda) + sin(\alpha)sin(\vartheta)$, $B(\lambda) = \sqrt{1 - C^2(\lambda)}$, and $C(\lambda) = sin(\alpha)D(\lambda) - cos(\alpha)sin(\vartheta)$ [43]. Figure 2(B) shows the assessment of the first ten chromatic dispersion orders of a CaF_2 prism-pair compressor for a UV laser pulse with a central wavelength $\lambda_L = 0.4\ \mu m$ and a spectral bandwidth $\Delta\lambda = 30\ nm$, used near the Brewster incident angle $\vartheta_B = atan(n(\lambda_L))$. The compressor is constructed from commercially available prisms optimized for near 0.78 μm laser wavelength with an apex angle of the prisms $\alpha = \pi - 2\vartheta_B = 69.9°$. In this configuration, the incident angle $\vartheta = asin(n(\lambda_L)sin(\alpha/2))$ is insignificantly deviated by approximately 0.4° from the Brewster angle for $\lambda_L = 0.4\ \mu m$. The dispersion orders are evaluated for the following parameters: a normal distance between the prisms $L = 30\ cm$, a prism length $\ell = 30\ mm$, a range of insertion depths of the first prism $\ell_1 = 1 - 15\ mm$, and a near-minimal insertion depth of the second prism $\ell_2 = 1\ mm$ at the shortest wavelength $\lambda_m = \lambda_L - \Delta\lambda/2$. The insertion depth ℓ_2 promotes further finer adjustment of the dispersion. We note that for a broadband laser pulse with a central wavelength of 0.4 μm, the higher material dispersion orders $p \geqslant 3$ are very small and positive, except for the material dispersion of the eighth and the tenth or the higher even orders, which are negative for CaF_2 (Fig. 1(A)). In an intuitive picture, the combination of the UV material dispersion and the negative angular dispersion of the prisms results in a positive dispersion slope as a function of the increasing insertion length of Prism 1, for the second through the

Optics EXPRESS

seventh, and the ninth compressor dispersion orders for which the material dispersion per unit length is positive. Interestingly, the eighth and the tenth compressor dispersion orders exhibit negative dispersion slopes as their material dispersion is negative. Furthermore, these slopes are very small for the high orders of dispersion of the compressor, owing to which the UV pulse compression is not excessively sensitive to these orders with the insertion lengths of the prisms. In conventional near-IR–mid-IR prism-pair compressors, the negative and positive slopes of the compressor dispersion are somewhat more strongly pronounced due to the large spread of the even and the odd material dispersion orders and their larger magnitudes.

Finally, we analyze the dispersion performance of photonic bandgap-like hollow-core fibers with a revolver substructure (Fig. 3(B)) [45]. These anti-resonant waveguides have been envisioned as a potential substitute for the present-day telecommunication network fibers and as components for various advanced photonic devices. We evaluate the waveguide chromatic dispersion orders assuming a complex wavevector $k(\lambda) = \frac{\omega}{c} n_{eff}^{ij}(\lambda)$ and an effective refractive index n_{eff}^{11} for the fundamental linearly polarized hybrid HE_{11} mode. To considerably reduce the attenuation, we couple a free-space linearly polarized Gaussian laser mode to this lowest-loss waveguide mode. The real part of the effective refractive index for the hybrid modes HE_{ij} to a first order approximation can be expressed as: $Re\left(n_{eff}^{ij}\right) \cong n_0 - \frac{1}{2n_0}\left(\frac{u_{ij}}{k_0 R}\right)^2 - \frac{u_{ij}^2}{2(k_0 n_0 R)^3}\frac{n^2+n_0^2}{\sqrt{n^2-n_0^2}}cot(\phi)$, where n_0 is the refractive index of the hollow-core, n is the refractive index of the fiber material, $k_0 = 2\pi/\lambda$, R is the radius of the inner hollow-core, ℓ is the thickness of the inner tubes, $\phi = k_0 \ell \sqrt{n^2 - n_0^2}$ is the phase controlling the resonant behavior, and u_{ij} is the j^{th} zero of the Bessel function of the first kind $J_{i-1}(x)$, ($u_{11} \cong 2.40483$) [45]. The attenuation for the hybrid modes HE_{ij} to a first order approximation is: $\alpha\left[\frac{dB}{m}\right] \cong 8.686\frac{(1+cot^2(\phi))\left(n^4+n_0^4\right)u_{ij}^3}{2(n^2-n_0^2)k_0^3 n_0^5 R^4}$, which can be designed to have a considerably smaller absorption compared to that of a regular hollow-core waveguide (λ^2/R^3 characteristic attenuation) [46,47].

As a next level of optimization, hollow-core fibers can potentially offer a larger bit-rate-length transfer product considering that light propagates faster in air than in a glass core which is currently used in modern telecommunication networks. In addition, these classes of hollow fibers can withstand high energies and maintain a pure polarization state [48]. However, the attenuation levels and the varying ambient air density have adverse effects.

The first ten waveguide dispersion orders of the HE_{11} mode of a photonic structure made of fused silica glass are presented in Fig. 3(A) for the transparent spectral band between 0.21 μm and 6.7 μm [32,49,50]. The anti-resonant fiber with an inner radius $R = 30$ μm and a revolver wall thickness of $\ell = 300$ nm is placed in vacuum ($n_0 = 1$). At the zero-dispersion GDD wavelengths of the waveguide, this geometry has a dominant third-order dispersion, which is lower than the material dispersion of fused silica. The analyses indicate that the values of the high orders of dispersion for $\ell = 300$ nm are relatively larger than the corresponding material dispersion orders because the curves pass through discontinuities. However, decreasing ℓ can reduce the number of resonances, the spectral interval in which all the even orders are zero, and the values of the dispersion order. Equivalently, both the dispersion values and the attenuation decrease for shorter laser wavelengths in the UV region owing to a smaller λ/R ratio. In applications in which these structured fibers are used as a precursor for self-guiding via filamentation or for guiding of long femtosecond-to-picosecond pulses over relatively short distances, these effects can be of lesser concern, for example, in laser pulse compression, spectral broadening, high harmonic generation, etc.

Here, the general trend of the effective refractive index of this class of anti-resonant fibers is a series of material-like absorptive resonances with monotonically decreasing functional form in-between towards the longer wavelengths. The wall thickness ℓ of the revolver capillaries for a given inner radius R can be changed to control the number of resonance discontinuities of the

Optics EXPRESS

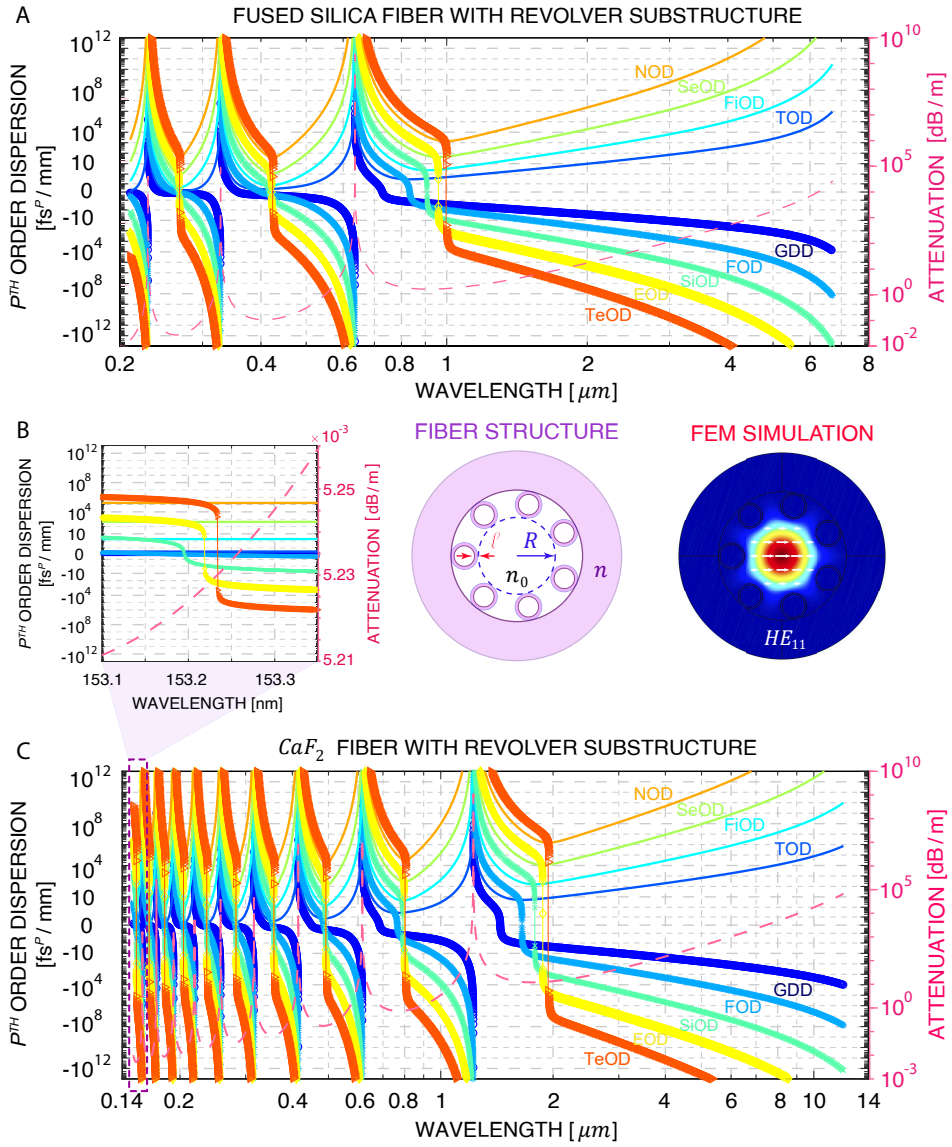

Fig. 3. High chromatic dispersion orders in anti-resonant hollow-core fibers in the UV, VIS, and IR spectral regions. Chromatic dispersion up to the tenth order, $2 \leq p \leq 10$, for a photonic band-gap fiber with an inner revolver substructure of $R = 30\ \mu m$, made of A) fused silica with a wall thickness of $\ell = 300\ nm$, and C) CaF_2 of lower chromatic dispersion with a larger wall thickness of $\ell = 600\ nm$. The attenuation is plotted in a dashed red-rose color. B) Dispersion in the deep UV region near 153 nm for a CaF_2 structured fiber showing the closely spaced zeros of the even orders (within 0.05 nm), and the very small values of all dispersion orders. Insets: Schematics of the substructure of the anti-resonant fibers, as well as the considered linearly polarized fundamental HE_{11} mode, calculated using the Finite Element Method (FEM). The arrows indicate the electric field polarization of the mode.

Optics EXPRESS

dispersion, the attenuation, and the spectral interval width within which all the even orders are zero. Moreover, the thickness ℓ affects the zero-dispersion wavelength of the *GDD* and all other even dispersion orders, which can be displaced towards or away from a central laser wavelength (Fig. 3(A), 3(B), and 3(C)). The resonances introduce multiple characteristic zero-dispersion wavelengths for all even orders at the inflection points, which can be tuned further by introducing atomic or molecular gas density for pulse self-compression applications. The analyses highlight that the odd orders are strictly positive and decrease towards the UV region, whereas the even orders exhibit step-like behavior and cross the zero line accompanied by a change in sign. The *GDD* is positive and negative on the left and right-hand sides of the zero *GDD* dispersion point, respectively, and this framework can enable self-compression to few-cycle pulse durations for spectrally broadened pulses in gas-filled fibers.

Additionally, we assess a novel class of non-fused-silica-based fibers made of CaF_2 in its broad, highly transparent spectral window of $0.15 - 12\ \mu m$ [32,33,51]. For comparison, we consider a fiber with the same inner radius $R = 30\ \mu m$ but with a larger wall thickness of $\ell = 600\ nm$ to emphasize the closely spaced zero-dispersion points of all even dispersion orders, Fig. 3(B). The lower values of dispersion of CaF_2 help ensure that the magnitude of the dispersion is smaller for larger ℓ, which are also less technologically challenging, while expanding the operational bandwidth in the vacuum UV and mid-IR ranges. Figure 3(C) highlights the similar characteristic behavior of the first ten orders, although with a larger number of discontinuities compared to that in fused silica. Remarkably, in the vacuum UV region, the zero-dispersion wavelengths for all even orders are spread only within less than 0.05 *nm*, near 153.2 *nm* with a leading fifth order and extremely small other higher orders, as shown in the inset of Fig. 3(B). Narrow-band laser pulse guiding or data transmission may be advantageous at many of these multiple locations due to minimal low and high order dispersion, as well as minimal attenuation when using UV or VIS pulses that are not significantly affected by the high dispersion orders. However, gas dispersion can have adverse effects.

In perspective, the attenuation of these classes of anti-resonant fibers is now approaching the challenging level of attenuation in the telecommunication industry [52]. Combined with their unique tunability and distinctive dispersion advantages, these fibers might be even used for data transmission in the near future, along with many other ultrafast femtosecond applications.

4. Conclusions

In summary, we present a general analytical formalism in Lah-Laguerre optics for the chromatic dispersion and dispersion slope parameters of advanced ultrafast optical systems. We identify polynomial and recursive relations for the chromatic dispersion orders based on the Lah and Laguerre transforms. These transforms are hypergeometric series that are computationally very efficient and can minimize the error of the analyses. The derived recursive relationships for the polynomials $G_p^{(\alpha)}$ that describe the dispersion orders are of particular interest when the phase derivatives are repetitive. In general, the described formalism is applicable to analyses of material and geometrical dispersion of ultrafast pulse space-time dynamics, of stretchers and compressors, advanced photonic fibers, or any dispersion of an optical system with a well-characterized frequency-dependent phase. Additionally, we explicitly list the closed-form dispersion relations and dispersion slope parameters for the first ten dispersion orders, for the first time. Using this analytical formalism, the computational time to evaluate all high chromatic orders up to the p^{th} order can be minimized as much as $(p-1)!$ times, compared to that associated with the use of chain sequences of the form: $\frac{\partial^{p+1}}{\partial\omega^{p+1}}\varphi(\omega) = \left(-\frac{\lambda^2}{2\pi c}\right)\frac{\partial}{\partial\lambda}\left(\frac{\partial^p}{\partial\omega^p}\varphi(\omega)\right)$. Although the formulated relations may introduce uncertainties in the chromatic dispersion owing to experimental errors in the measurements of the refractive index, this analytical formalism can be used in reverse to enhance the precision of the refractive index measurements. Further, a desired phase and

Optics EXPRESS

dispersion can be attained in reverse by optimization of the properties of novel materials and optical systems. The very high orders of the chromatic dispersion become significant at large propagation lengths, as in state-of-the-art ultrafast laser amplifiers, or when the spectral content of the pulses spans an octave, as in single-cycle ultrafast laser pulse generation. Our analyses indicate that in spectral regions with low values of the high dispersion orders, most often in the UV spectral region, the induced phase changes in materials, ultrafast single-cycle laser pulse propagation, photonic fiber designs, etc., are not significantly sensitive to the high orders of dispersion, and a near-transform-limited pulse compression or any phase compensation can be easily achieved by balancing fewer orders compared to those in the near-IR–mid-IR region.

In perspective, to minimize the computational intensity, for phases specified as discrete values, the data can be first fitted to a smooth differentiable function before proceeding in the usual manner by using Eq. (12). Further gain in computational efficiency can be accomplished by using simplified fitting functions or parallel computing. Numerically, the highest order of dispersion that can be evaluated is limited by the computer architecture's ability to allocate the smallest and largest floating-point number. Lastly, the evaluation of the high orders of dispersion at or away from the zero *GDD* dispersion wavelength is computationally fast, making compensation optimization of the dispersion orders an efficient procedure for any complex ultrafast optical design.

In the following appendices, we list for reference the closed-form expressions and the relevant matrix elements in Lah-Laguerre optics discussed throughout the main text.

Appendix A. Forward and inverse transforms for the chromatic dispersion orders as a function of frequency

The chromatic dispersion equations for the wavevector $k(\omega) = \frac{\omega}{c} n(\omega)$ and the phase $\varphi(\omega) = \frac{\omega}{c} OP(\omega)$ (Eqs. (4) and (5), respectively) have the same functional form. In general:

$$\frac{\partial^p}{\partial \omega^p}\left(\frac{\omega}{c} f(\omega)\right) = \frac{1}{c}\left(p\frac{\partial^{p-1}}{\partial \omega^{p-1}} f(\omega) + \omega \frac{\partial^p}{\partial \omega^p} f(\omega)\right) = \frac{\omega^{1-p}}{c}\sum_{m=0}^{p} \mathcal{V}(p,m)\omega^m \frac{\partial^m}{\partial \omega^m} f(\omega) \tag{31}$$

The inverse transform yields the Taylor coefficients of the refractive index from the phase in the frequency domain:

$$\omega^p \frac{\partial^p}{\partial \omega^p} f(\omega) = (-1)^p \frac{c}{\omega} \sum_{m=0}^{p} \mathcal{V}(p,m)^{-1} \omega^m \frac{\partial^m}{\partial \omega^m}\left(\frac{\omega}{c} f(\omega)\right) \tag{32}$$

Table 1. Matrix elements $\mathcal{V}(p, m)$ up to the tenth order.

Dispersion order p		$d_\lambda^{(0)}$ $m=0$	$d_\lambda^{(1)}$ $m=1$	$d_\lambda^{(2)}$ $m=2$	$d_\lambda^{(3)}$ $m=3$	$d_\lambda^{(4)}$ $m=4$	$d_\lambda^{(5)}$ $m=5$	$d_\lambda^{(6)}$ $m=6$	$d_\lambda^{(7)}$ $m=7$	$d_\lambda^{(8)}$ $m=8$	$d_\lambda^{(9)}$ $m=9$	$d_\lambda^{(10)}$ $m=10$
First	$p=1$	1	1	0	0	0	0	0	0	0	0	0
Second	$p=2$	0	2	1	0	0	0	0	0	0	0	0
Third	$p=3$	0	0	3	1	0	0	0	0	0	0	0
Fourth	$p=4$	0	0	0	4	1	0	0	0	0	0	0
Fifth	$p=5$	0	0	0	0	5	1	0	0	0	0	0
Sixth	$p=6$	0	0	0	0	0	6	1	0	0	0	0
Seventh	$p=7$	0	0	0	0	0	0	7	1	0	0	0
Eight	$p=8$	0	0	0	0	0	0	0	8	1	0	0
Ninth	$p=9$	0	0	0	0	0	0	0	0	9	1	0
Tenth	$p=10$	0	0	0	0	0	0	0	0	0	10	1

Optics EXPRESS

where $f(\omega)$ represents either the refractive index n or the optical path OP, and the matrix coefficients $\mathcal{V}(p,m) = p\delta_{p-1,m} + \delta_{p,m}$ are listed in Table 1. The inverse matrix elements $\mathcal{V}(p,m)^{-1} = (-1)^m \frac{p!}{m!}$ are identical to the $\mathcal{E}(p,m)$ coefficients, listed in Table 6, Appendix E. $\delta_{p,m}$ represents the Kronecker delta with values $\delta_{p,m} = 1$ if $p = m$, and 0 otherwise.

For completeness, the first ten dispersion orders, written for the wavevector, are expressed as a function of frequency, as:

$$\text{A I. } \frac{\partial}{\partial\omega}k(\omega) = \frac{1}{c}\left(n(\omega) + \omega\frac{\partial n(\omega)}{\partial\omega}\right) \qquad \text{A II. } \frac{\partial^2}{\partial\omega^2}k(\omega) = \frac{1}{c}\left(2\frac{\partial n(\omega)}{\partial\omega} + \omega\frac{\partial^2 n(\omega)}{\partial\omega^2}\right) \tag{33}$$

$$\text{A III. } \frac{\partial^3}{\partial\omega^3}k(\omega) = \frac{1}{c}\left(3\frac{\partial^2 n(\omega)}{\partial\omega^2} + \omega\frac{\partial^3 n(\omega)}{\partial\omega^3}\right) \qquad \text{A IV. } \frac{\partial^4}{\partial\omega^4}k(\omega) = \frac{1}{c}\left(4\frac{\partial^3 n(\omega)}{\partial\omega^3} + \omega\frac{\partial^4 n(\omega)}{\partial\omega^4}\right) \tag{34}$$

$$\text{A V. } \frac{\partial^5}{\partial\omega^5}k(\omega) = \frac{1}{c}\left(5\frac{\partial^4 n(\omega)}{\partial\omega^4} + \omega\frac{\partial^5 n(\omega)}{\partial\omega^5}\right) \qquad \text{A VI. } \frac{\partial^6}{\partial\omega^6}k(\omega) = \frac{1}{c}\left(6\frac{\partial^5 n(\omega)}{\partial\omega^5} + \omega\frac{\partial^6 n(\omega)}{\partial\omega^6}\right) \tag{35}$$

$$\text{A VII. } \frac{\partial^7}{\partial\omega^7}k(\omega) = \frac{1}{c}\left(7\frac{\partial^6 n(\omega)}{\partial\omega^6} + \omega\frac{\partial^7 n(\omega)}{\partial\omega^7}\right) \qquad \text{A VIII. } \frac{\partial^8}{\partial\omega^8}k(\omega) = \frac{1}{c}\left(8\frac{\partial^7 n(\omega)}{\partial\omega^7} + \omega\frac{\partial^8 n(\omega)}{\partial\omega^8}\right) \tag{36}$$

$$\text{A IX. } \frac{\partial^9}{\partial\omega^9}k(\omega) = \frac{1}{c}\left(9\frac{\partial^8 n(\omega)}{\partial\omega^8} + \omega\frac{\partial^9 n(\omega)}{\partial\omega^9}\right) \qquad \text{A X. } \frac{\partial^{10}}{\partial\omega^{10}}k(\omega) = \frac{1}{c}\left(10\frac{\partial^9 n(\omega)}{\partial\omega^9} + \omega\frac{\partial^{10} n(\omega)}{\partial\omega^{10}}\right) \tag{37}$$

Appendix B. Lah transforms for the chromatic dispersion orders and chromatic dispersion orders of the phase

The derivatives of any function $f(\omega|\lambda)$ in the wavelength or the frequency space, as in Eqs. (6), (10) and (12), can be generalized using the forward and inverse Lah transforms as:

$$\frac{\partial^p}{\partial\omega^p}f(\omega) = (-1)^p\left(\frac{\lambda}{2\pi c}\right)^p \sum_{m=0}^{p} \mathcal{A}(p,m)\lambda^m \frac{\partial^m}{\partial\lambda^m}f(\lambda) \tag{38}$$

$$\frac{\partial^p}{\partial\lambda^p}f(\lambda) = (-1)^p\left(\frac{\omega}{2\pi c}\right)^p \sum_{m=0}^{p} \mathcal{A}(p,m)\omega^m \frac{\partial^m}{\partial\omega^m}f(\omega) \tag{39}$$

The phase $\varphi(\omega|\lambda)$, the refractive index $n(\omega|\lambda)$, the optical path $OP(\omega|\lambda)$, the group delay $\tau_g(\omega|\lambda)$ and any differentiable function $f(\omega|\lambda)$ can be used interchangeably in the frequency-wavelength Lah transforms. The relevant matrix elements $\mathcal{A}(p,m) = \frac{p!}{(p-m)!m!}\frac{(p-1)!}{(m-1)!}$ are listed

Table 2. Matrix elements $\mathcal{A}(p,m)$ and Lah numbers up to the tenth order.

Derivative order p	$d_\lambda^{(1)}$ $m=1$	$d_\lambda^{(2)}$ $m=2$	$d_\lambda^{(3)}$ $m=3$	$d_\lambda^{(4)}$ $m=4$	$d_\lambda^{(5)}$ $m=5$	$d_\lambda^{(6)}$ $m=6$	$d_\lambda^{(7)}$ $m=7$	$d_\lambda^{(8)}$ $m=8$	$d_\lambda^{(9)}$ $m=9$	$d_\lambda^{(10)}$ $m=10$
First $p=1$	1	0	0	0	0	0	0	0	0	0
Second $p=2$	2	1	0	0	0	0	0	0	0	0
Third $p=3$	6	6	1	0	0	0	0	0	0	0
Fourth $p=4$	24	36	12	1	0	0	0	0	0	0
Fifth $p=5$	120	240	120	20	1	0	0	0	0	0
Sixth $p=6$	720	1800	1200	300	30	1	0	0	0	0
Seventh $p=7$	5040	15120	12600	4200	630	42	1	0	0	0
Eight $p=8$	40320	141120	141120	58800	11760	1176	56	1	0	0
Ninth $p=9$	362880	1451520	1693440	846720	211680	28224	2016	72	1	0
Tenth $p=10$	3628800	16329600	21772800	12700800	3810240	635040	60480	3240	90	1

Optics EXPRESS

in Table 2. For $p = 0$, the binomials with negative arguments are set as $\binom{-n}{k} = (-1)^k \binom{n}{k}$ and 0 for $n<k<0$. Thus, the non-zero element for $p<1$ is $\mathcal{A}(0,0) = 1$. The Lah transform is also a Laguerre transform of order negative one, $\alpha = -1$.

Written for the phase φ, the first ten dispersion orders can be expressed as a function of wavelength using the Lah transforms as:

$$\text{B I.}\ \frac{\partial\varphi(\omega)}{\partial\omega} = -\left(\frac{\lambda}{2\pi c}\right) G_1^{(-1)}(\lambda) = -\left(\frac{2\pi c}{\omega^2}\right)\frac{\partial\varphi(\omega)}{\partial\lambda} = -\left(\frac{\lambda^2}{2\pi c}\right)\frac{\partial\varphi(\lambda)}{\partial\lambda} \tag{40}$$

$$\text{B II.}\ \frac{\partial^2\varphi(\omega)}{\partial\omega^2} = \frac{\partial}{\partial\omega}\left(\frac{\partial\varphi(\omega)}{\partial\omega}\right) = \left(\frac{\lambda}{2\pi c}\right)^2 G_2^{(-1)}(\lambda) = \left(\frac{\lambda}{2\pi c}\right)^2\left(2\lambda\frac{\partial\varphi(\lambda)}{\partial\lambda} + \lambda^2\frac{\partial^2\varphi(\lambda)}{\partial\lambda^2}\right) \tag{41}$$

$$\text{B III.}\ \frac{\partial^3\varphi(\omega)}{\partial\omega^3} = -\left(\frac{\lambda}{2\pi c}\right)^3 G_3^{(-1)}(\lambda) = -\left(\frac{\lambda}{2\pi c}\right)^3\left(6\lambda\frac{\partial\varphi(\lambda)}{\partial\lambda} + 6\lambda^2\frac{\partial^2\varphi(\lambda)}{\partial\lambda^2} + \lambda^3\frac{\partial^3\varphi(\lambda)}{\partial\lambda^3}\right) \tag{42}$$

$$\text{B IV.}\ \frac{\partial^4\varphi(\omega)}{\partial\omega^4} = \left(\frac{\lambda}{2\pi c}\right)^4 G_4^{(-1)}(\lambda) = \left(\frac{\lambda}{2\pi c}\right)^4\left(24\lambda\frac{\partial\varphi(\lambda)}{\partial\lambda} + 36\lambda^2\frac{\partial^2\varphi(\lambda)}{\partial\lambda^2} + 12\lambda^3\frac{\partial^3\varphi(\lambda)}{\partial\lambda^3} + \right. \\ \left. + \lambda^4\frac{\partial^4\varphi(\lambda)}{\partial\lambda^4}\right) \tag{43}$$

$$\text{B V.}\ \frac{\partial^5\varphi(\omega)}{\partial\omega^5} = -\left(\frac{\lambda}{2\pi c}\right)^5 G_5^{(-1)}(\lambda) = -\left(\frac{\lambda}{2\pi c}\right)^5\left(120\lambda\frac{\partial\varphi(\lambda)}{\partial\lambda} + 240\lambda^2\frac{\partial^2\varphi(\lambda)}{\partial\lambda^2} + \right. \\ \left. + 120\lambda^3\frac{\partial^3\varphi(\lambda)}{\partial\lambda^3} + 20\lambda^4\frac{\partial^4\varphi(\lambda)}{\partial\lambda^4} + \lambda^5\frac{\partial^5\varphi(\lambda)}{\partial\lambda^5}\right) \tag{44}$$

$$\text{B VI.}\ \frac{\partial^6\varphi(\omega)}{\partial\omega^6} = \left(\frac{\lambda}{2\pi c}\right)^6 G_6^{(-1)}(\lambda) = \left(\frac{\lambda}{2\pi c}\right)^6\left(720\lambda\frac{\partial\varphi(\lambda)}{\partial\lambda} + 1800\lambda^2\frac{\partial^2\varphi(\lambda)}{\partial\lambda^2} + \right. \\ \left. + 1200\lambda^3\frac{\partial^3\varphi(\lambda)}{\partial\lambda^3} + 300\lambda^4\frac{\partial^4\varphi(\lambda)}{\partial\lambda^4} + 30\lambda^5\frac{\partial^5\varphi(\lambda)}{\partial\lambda^5} + \lambda^6\frac{\partial^6\varphi(\lambda)}{\partial\lambda^6}\right) \tag{45}$$

$$\text{B VII.}\ \frac{\partial^7\varphi(\omega)}{\partial\omega^7} = -\left(\frac{\lambda}{2\pi c}\right)^7 G_7^{(-1)}(\lambda) = -\left(\frac{\lambda}{2\pi c}\right)^7\left(5040\lambda\frac{\partial\varphi(\lambda)}{\partial\lambda} + 15120\lambda^2\frac{\partial^2\varphi(\lambda)}{\partial\lambda^2} + \right. \\ \left. + 12600\lambda^3\frac{\partial^3\varphi(\lambda)}{\partial\lambda^3} + 4200\lambda^4\frac{\partial^4\varphi(\lambda)}{\partial\lambda^4} + 630\lambda^5\frac{\partial^5\varphi(\lambda)}{\partial\lambda^5} + 42\lambda^6\frac{\partial^6\varphi(\lambda)}{\partial\lambda^6} + \lambda^7\frac{\partial^7\varphi(\lambda)}{\partial\lambda^7}\right) \tag{46}$$

$$\text{B VIII.}\ \frac{\partial^8\varphi(\omega)}{\partial\omega^8} = \left(\frac{\lambda}{2\pi c}\right)^8 G_8^{(-1)}(\lambda) = \left(\frac{\lambda}{2\pi c}\right)^8\left(40320\lambda\frac{\partial\varphi(\lambda)}{\partial\lambda} + 141120\lambda^2\frac{\partial^2\varphi(\lambda)}{\partial\lambda^2} + \right. \\ \left. + 141120\lambda^3\frac{\partial^3\varphi(\lambda)}{\partial\lambda^3} + 58800\lambda^4\frac{\partial^4\varphi(\lambda)}{\partial\lambda^4} + 11760\lambda^5\frac{\partial^5\varphi(\lambda)}{\partial\lambda^5} + 1176\lambda^6\frac{\partial^6\varphi(\lambda)}{\partial\lambda^6} + \right. \\ \left. + 56\lambda^7\frac{\partial^7\varphi(\lambda)}{\partial\lambda^7} + \lambda^8\frac{\partial^8\varphi(\lambda)}{\partial\lambda^8}\right) \tag{47}$$

Optics EXPRESS

$$\text{B IX. } \frac{\partial^9\varphi(\omega)}{\partial\omega^9} = -\left(\frac{\lambda}{2\pi c}\right)^9 G_9^{(-1)}(\lambda) = -\left(\frac{\lambda}{2\pi c}\right)^9 \left(362880\lambda\frac{\partial\varphi(\lambda)}{\partial\lambda} + 1451520\lambda^2\frac{\partial^2\varphi(\lambda)}{\partial\lambda^2} + \right.$$
$$+ 1693440\lambda^3\frac{\partial^3\varphi(\lambda)}{\partial\lambda^3} + 846720\lambda^4\frac{\partial^4\varphi(\lambda)}{\partial\lambda^4} + 211680\lambda^5\frac{\partial^5\varphi(\lambda)}{\partial\lambda^5} + 28224\lambda^6\frac{\partial^6\varphi(\lambda)}{\partial\lambda^6} + \tag{48}$$
$$\left. + 2016\lambda^7\frac{\partial^7\varphi(\lambda)}{\partial\lambda^7} + 72\lambda^8\frac{\partial^8\varphi(\lambda)}{\partial\lambda^8} + \lambda^9\frac{\partial^9\varphi(\lambda)}{\partial\lambda^9}\right)$$
$$\text{B X. } \frac{\partial^{10}\varphi(\omega)}{\partial\omega^{10}} = \left(\frac{\lambda}{2\pi c}\right)^{10} G_{10}^{(-1)}(\lambda) = \left(\frac{\lambda}{2\pi c}\right)^{10} \left(3628800\lambda\frac{\partial\varphi(\lambda)}{\partial\lambda} + 16329600\lambda^2\frac{\partial^2\varphi(\lambda)}{\partial\lambda^2} + \right.$$
$$+ 21772800\lambda^3\frac{\partial^3\varphi(\lambda)}{\partial\lambda^3} + 12700800\lambda^4\frac{\partial^4\varphi(\lambda)}{\partial\lambda^4} + 3810240\lambda^5\frac{\partial^5\varphi(\lambda)}{\partial\lambda^5} + 635040\lambda^6\frac{\partial^6\varphi(\lambda)}{\partial\lambda^6} + \tag{49}$$
$$\left. + 60480\lambda^7\frac{\partial^7\varphi(\lambda)}{\partial\lambda^7} + 3240\lambda^8\frac{\partial^8\varphi(\lambda)}{\partial\lambda^8} + 90\lambda^9\frac{\partial^9\varphi(\lambda)}{\partial\lambda^9} + \lambda^{10}\frac{\partial^{10}\varphi(\lambda)}{\partial\lambda^{10}}\right)$$

Appendix C. Chromatic dispersion orders and Laguerre transforms for the chromatic dispersion orders

The dispersion orders in Eqs. (15) and (16) are generalized through a Laguerre type transform of order negative two, $\alpha = -2$:

$$POD(n) = \frac{\partial^p}{\partial\omega^p}k(\omega) = (-1)^p\frac{1}{c}\left(\frac{\lambda}{2\pi c}\right)^{p-1}\sum_{m=0}^{p}\mathcal{B}(p,m)\,\lambda^m\frac{\partial^m}{\partial\lambda^m}n(\lambda) \tag{50}$$

$$POD(OP) = \frac{\partial^p}{\partial\omega^p}\varphi(\omega) = (-1)^p\frac{1}{c}\left(\frac{\lambda}{2\pi c}\right)^{p-1}\sum_{m=0}^{p}\mathcal{B}(p,m)\,\lambda^m\frac{\partial^m}{\partial\lambda^m}OP(\lambda) \tag{51}$$

The inverse transforms relate the Taylor coefficients of the refractive index or the optical path to the wavevector or the phase:

$$\lambda^p\frac{\partial^p}{\partial\lambda^p}n(\lambda) = (-1)^p\frac{c}{\omega}\sum_{m=0}^{p}\mathcal{B}(p,m)\omega^m\frac{\partial^m}{\partial\omega^m}k(\omega) \tag{52}$$

$$\lambda^p\frac{\partial^p}{\partial\lambda^p}OP(\lambda) = (-1)^p\frac{c}{\omega}\sum_{m=0}^{p}\mathcal{B}(p,m)\omega^m\frac{\partial^m}{\partial\omega^m}\varphi(\omega) \tag{53}$$

Table 3. Matrix elements $\mathcal{B}(p,m)$ up to the tenth order and unsigned Laguerre coefficients for $\alpha = -2$.

Dispersion order p	$d_\lambda^{(2)}$ $m=2$	$d_\lambda^{(3)}$ $m=3$	$d_\lambda^{(4)}$ $m=4$	$d_\lambda^{(5)}$ $m=5$	$d_\lambda^{(6)}$ $m=6$	$d_\lambda^{(7)}$ $m=7$	$d_\lambda^{(8)}$ $m=8$	$d_\lambda^{(9)}$ $m=9$	$d_\lambda^{(10)}$ $m=10$
Second $p=2$	1	0	0	0	0	0	0	0	0
Third $p=3$	3	1	0	0	0	0	0	0	0
Fourth $p=4$	12	8	1	0	0	0	0	0	0
Fifth $p=5$	60	60	15	1	0	0	0	0	0
Sixth $p=6$	360	480	180	24	1	0	0	0	0
Seventh $p=7$	2520	4200	2100	420	35	1	0	0	0
Eight $p=8$	20160	40320	25200	6720	840	48	1	0	0
Ninth $p=9$	181440	423360	317520	105840	17640	1512	63	1	0
Tenth $p=10$	1814400	4838400	4233600	1693440	352800	40320	2520	80	1

Optics EXPRESS

The matrix elements of the transforms $\mathcal{B}(p,m) = \frac{p!}{(p-m)!m!}\frac{(p-2)!}{(m-2)!}$ are listed in Table 3. For $p = 0$ and $p = 1$, the binomials with negative arguments are evaluated as $\binom{-n}{k} = (-1)^k\binom{n}{k}$ and 0 for $n<k<0$. Thus, the non-zero block of matrix elements for $p<2$ are $\mathcal{B}(0,0) = 1$, $\mathcal{B}(1,0) = -1$, and $\mathcal{B}(1,1) = 1$.

The first four chromatic dispersion orders are well-known in the literature. Using the above-mentioned Lah-Laguerre optical formalism, the first ten dispersion orders, written for the wavevector, can be explicitly written in closed-form expressions as:

$$\text{C I. } \boldsymbol{GD} = \frac{\partial}{\partial\omega}k(\omega) = \frac{1}{c}\left(n(\omega) + \omega\frac{\partial n(\omega)}{\partial\omega}\right) = -\frac{1}{c}G_1^{(-2)}(\lambda) = \frac{1}{c}\left(n(\lambda) - \lambda\frac{\partial n(\lambda)}{\partial\lambda}\right) = v_{gr}^{-1} \tag{54}$$

The group refractive index n_g is defined in terms of the group velocity v_{gr}: $n_g = cv_{gr}^{-1}$.

$$\begin{aligned}&\text{C II. } \boldsymbol{GDD} = \frac{\partial^2}{\partial\omega^2}k(\omega) = \frac{1}{c}\left(2\frac{\partial n(\omega)}{\partial\omega} + \omega\frac{\partial^2 n(\omega)}{\partial\omega^2}\right) = \frac{1}{c}\left(\frac{\lambda}{2\pi c}\right)G_2^{(-2)}(\lambda) = \\ &= \frac{1}{c}\left(\frac{\lambda}{2\pi c}\right)\left(\lambda^2\frac{\partial^2 n(\lambda)}{\partial\lambda^2}\right)\end{aligned} \tag{55}$$

$$\begin{aligned}&\text{C III. } \boldsymbol{TOD} = \frac{\partial^3}{\partial\omega^3}k(\omega) = \frac{1}{c}\left(3\frac{\partial^2 n(\omega)}{\partial\omega^2} + \omega\frac{\partial^3 n(\omega)}{\partial\omega^3}\right) = -\frac{1}{c}\left(\frac{\lambda}{2\pi c}\right)^2 G_3^{(-2)}(\lambda) = \\ &= -\frac{1}{c}\left(\frac{\lambda}{2\pi c}\right)^2\left(3\lambda^2\frac{\partial^2 n(\lambda)}{\partial\lambda^2} + \lambda^3\frac{\partial^3 n(\lambda)}{\partial\lambda^3}\right)\end{aligned} \tag{56}$$

$$\begin{aligned}&\text{C IV. } \boldsymbol{FOD} = \frac{\partial^4}{\partial\omega^4}k(\omega) = \frac{1}{c}\left(4\frac{\partial^3 n(\omega)}{\partial\omega^3} + \omega\frac{\partial^4 n(\omega)}{\partial\omega^4}\right) = \frac{1}{c}\left(\frac{\lambda}{2\pi c}\right)^3 G_4^{(-2)}(\lambda) = \\ &= \frac{1}{c}\left(\frac{\lambda}{2\pi c}\right)^3\left(12\lambda^2\frac{\partial^2 n(\lambda)}{\partial\lambda^2} + 8\lambda^3\frac{\partial^3 n(\lambda)}{\partial\lambda^3} + \lambda^4\frac{\partial^4 n(\lambda)}{\partial\lambda^4}\right)\end{aligned} \tag{57}$$

$$\begin{aligned}&\text{C V. } \boldsymbol{FiOD} = \frac{\partial^5}{\partial\omega^5}k(\omega) = \frac{1}{c}\left(5\frac{\partial^4 n(\omega)}{\partial\omega^4} + \omega\frac{\partial^5 n(\omega)}{\partial\omega^5}\right) = -\frac{1}{c}\left(\frac{\lambda}{2\pi c}\right)^4 G_5^{(-2)}(\lambda) = \\ &= -\frac{1}{c}\left(\frac{\lambda}{2\pi c}\right)^4\left(60\lambda^2\frac{\partial^2 n(\lambda)}{\partial\lambda^2} + 60\lambda^3\frac{\partial^3 n(\lambda)}{\partial\lambda^3} + 15\lambda^4\frac{\partial^4 n(\lambda)}{\partial\lambda^4} + \lambda^5\frac{\partial^5 n(\lambda)}{\partial\lambda^5}\right)\end{aligned} \tag{58}$$

$$\begin{aligned}&\text{C VI. } \boldsymbol{SiOD} = \frac{\partial^6}{\partial\omega^6}k(\omega) = \frac{1}{c}\left(6\frac{\partial^5 n(\omega)}{\partial\omega^5} + \omega\frac{\partial^6 n(\omega)}{\partial\omega^6}\right) = \frac{1}{c}\left(\frac{\lambda}{2\pi c}\right)^5 G_6^{(-2)}(\lambda) = \\ &= \frac{1}{c}\left(\frac{\lambda}{2\pi c}\right)^5\left(360\lambda^2\frac{\partial^2 n(\lambda)}{\partial\lambda^2} + 480\lambda^3\frac{\partial^3 n(\lambda)}{\partial\lambda^3} + 180\lambda^4\frac{\partial^4 n(\lambda)}{\partial\lambda^4} + \right. \\ &\left. + 24\lambda^5\frac{\partial^5 n(\lambda)}{\partial\lambda^5} + \lambda^6\frac{\partial^6 n(\lambda)}{\partial\lambda^6}\right)\end{aligned} \tag{59}$$

$$\begin{aligned}&\text{C VII. } \boldsymbol{SeOD} = \frac{\partial^7}{\partial\omega^7}k(\omega) = \frac{1}{c}\left(7\frac{\partial^6 n(\omega)}{\partial\omega^6} + \omega\frac{\partial^7 n(\omega)}{\partial\omega^7}\right) = -\frac{1}{c}\left(\frac{\lambda}{2\pi c}\right)^6 G_7^{(-2)}(\lambda) = \\ &= -\frac{1}{c}\left(\frac{\lambda}{2\pi c}\right)^6\left(2520\lambda^2\frac{\partial^2 n(\lambda)}{\partial\lambda^2} + 4200\lambda^3\frac{\partial^3 n(\lambda)}{\partial\lambda^3} + 2100\lambda^4\frac{\partial^4 n(\lambda)}{\partial\lambda^4} + 420\lambda^5\frac{\partial^5 n(\lambda)}{\partial\lambda^5} + \right. \\ &\left. + 35\lambda^6\frac{\partial^6 n(\lambda)}{\partial\lambda^6} + \lambda^7\frac{\partial^7 n(\lambda)}{\partial\lambda^7}\right)\end{aligned} \tag{60}$$

Optics EXPRESS

$$\text{C VIII. } \boldsymbol{EOD} = \frac{\partial^8}{\partial\omega^8}k(\omega) = \frac{1}{c}\left(8\frac{\partial^7 n(\omega)}{\partial\omega^7} + \omega\frac{\partial^8 n(\omega)}{\partial\omega^8}\right) = \frac{1}{c}\left(\frac{\lambda}{2\pi c}\right)^7 G_8^{(-2)}(\lambda) =$$
$$= \frac{1}{c}\left(\frac{\lambda}{2\pi c}\right)^7\left(20160\lambda^2\frac{\partial^2 n(\lambda)}{\partial\lambda^2} + 40320\lambda^3\frac{\partial^3 n(\lambda)}{\partial\lambda^3} + 25200\lambda^4\frac{\partial^4 n(\lambda)}{\partial\lambda^4} + 6720\lambda^5\frac{\partial^5 n(\lambda)}{\partial\lambda^5} + \right. \quad (61)$$
$$\left. + 840\lambda^6\frac{\partial^6 n(\lambda)}{\partial\lambda^6} + 48\lambda^7\frac{\partial^7 n(\lambda)}{\partial\lambda^7} + \lambda^8\frac{\partial^8 n(\lambda)}{\partial\lambda^8}\right)$$

$$\text{C IX. } \boldsymbol{NOD} = \frac{\partial^9}{\partial\omega^9}k(\omega) = \frac{1}{c}\left(9\frac{\partial^8 n(\omega)}{\partial\omega^8} + \omega\frac{\partial^9 n(\omega)}{\partial\omega^9}\right) = -\frac{1}{c}\left(\frac{\lambda}{2\pi c}\right)^8 G_9^{(-2)}(\lambda) =$$
$$= -\frac{1}{c}\left(\frac{\lambda}{2\pi c}\right)^8\left(181440\lambda^2\frac{\partial^2 n(\lambda)}{\partial\lambda^2} + 423360\lambda^3\frac{\partial^3 n(\lambda)}{\partial\lambda^3} + 317520\lambda^4\frac{\partial^4 n(\lambda)}{\partial\lambda^4} + \right. \quad (62)$$
$$\left. + 105840\lambda^5\frac{\partial^5 n(\lambda)}{\partial\lambda^5} + 17640\lambda^6\frac{\partial^6 n(\lambda)}{\partial\lambda^6} + 1512\lambda^7\frac{\partial^7 n(\lambda)}{\partial\lambda^7} + 63\lambda^8\frac{\partial^8 n(\lambda)}{\partial\lambda^8} + \lambda^9\frac{\partial^9 n(\lambda)}{\partial\lambda^9}\right)$$

$$\text{C X. } \boldsymbol{TeOD} = \frac{\partial^{10}}{\partial\omega^{10}}k(\omega) = \frac{1}{c}\left(10\frac{\partial^9 n(\omega)}{\partial\omega^9} + \omega\frac{\partial^{10} n(\omega)}{\partial\omega^{10}}\right) = \frac{1}{c}\left(\frac{\lambda}{2\pi c}\right)^9 G_{10}^{(-2)}(\lambda) =$$
$$= \frac{1}{c}\left(\frac{\lambda}{2\pi c}\right)^9\left(1814400\lambda^2\frac{\partial^2 n(\lambda)}{\partial\lambda^2} + 4838400\lambda^3\frac{\partial^3 n(\lambda)}{\partial\lambda^3} + 4233600\lambda^4\frac{\partial^4 n(\lambda)}{\partial\lambda^4} + \right. \quad (63)$$
$$+ 1693440\lambda^5\frac{\partial^5 n(\lambda)}{\partial\lambda^5} + 352800\lambda^6\frac{\partial^6 n(\lambda)}{\partial\lambda^6} + 40320\lambda^7\frac{\partial^7 n(\lambda)}{\partial\lambda^7} + 2520\lambda^8\frac{\partial^8 n(\lambda)}{\partial\lambda^8} +$$
$$\left. + 80\lambda^9\frac{\partial^9 n(\lambda)}{\partial\lambda^9} + \lambda^{10}\frac{\partial^{10} n(\lambda)}{\partial\lambda^{10}}\right)$$

Appendix D. Forward and inverse transforms for the dispersion slope parameters

The derivatives $\frac{\partial^p}{\partial\lambda^p}\tau_g$ or $\frac{\partial^p}{\partial\lambda^p}(v_{gr}^{-1})$ are often denoted as slopes of the dispersion parameters. The group velocity $v_{gr}^{-1} = \frac{1}{c}\left(n(\lambda) - \lambda\frac{\partial n(\lambda)}{\partial\lambda}\right)$ and group delay $\tau_g(\lambda) = zv_{gr}^{-1}$ can be used interchangeably in the equation for the slopes of the dispersion parameters (Eq. (25)), with the remark that the derivatives need to be expressed in terms of $n(\lambda)$ and $OP(\lambda)$, respectively:

$$\frac{\partial^p v_{gr}^{-1}(\lambda)}{\partial\lambda^p} = -\frac{1}{c}\left((p-1)\frac{\partial^p}{\partial\lambda^p}n(\lambda) + \lambda\frac{\partial^{p+1}}{\partial\lambda^{p+1}}n(\lambda)\right) = -\frac{1}{c}\lambda^{-p}\sum_{m=0}^{p+1}\mathcal{K}(p,m)\lambda^m\frac{\partial^m}{\partial\lambda^m}n(\lambda) \quad (64)$$

Table 4. Matrix elements $\mathcal{K}(p, m)$ up to the tenth order.

Dispersion order $p+1$		$d_\lambda^{(2)}$ $m=2$	$d_\lambda^{(3)}$ $m=3$	$d_\lambda^{(4)}$ $m=4$	$d_\lambda^{(5)}$ $m=5$	$d_\lambda^{(6)}$ $m=6$	$d_\lambda^{(7)}$ $m=7$	$d_\lambda^{(8)}$ $m=8$	$d_\lambda^{(9)}$ $m=9$	$d_\lambda^{(10)}$ $m=10$	$d_\lambda^{(11)}$ $m=11$
Second	$p=1$	1	0	0	0	0	0	0	0	0	0
Third	$p=2$	1	1	0	0	0	0	0	0	0	0
Fourth	$p=3$	0	2	1	0	0	0	0	0	0	0
Fifth	$p=4$	0	0	3	1	0	0	0	0	0	0
Sixth	$p=5$	0	0	0	4	1	0	0	0	0	0
Seventh	$p=6$	0	0	0	0	5	1	0	0	0	0
Eight	$p=7$	0	0	0	0	0	6	1	0	0	0
Ninth	$p=8$	0	0	0	0	0	0	7	1	0	0
Tenth	$p=9$	0	0	0	0	0	0	0	8	1	0
Eleventh	$p=10$	0	0	0	0	0	0	0	0	9	1

Optics EXPRESS

The corresponding matrix elements $\mathcal{K}(p,m) = (p-1)\delta_{p,m} + \delta_{p+1,m}$, ($\delta_{p,m} = 1$, if $p = m$ and 0 otherwise) are listed in Table 4.

The inverse transform relates the Taylor coefficients of the refractive index to the dispersion derivatives:

$$\lambda^p \frac{\partial^p}{\partial\lambda^p} n(\lambda) = (-1)^p c \sum_{m=0}^{p-1} \mathcal{K}(p,m)^{-1} \lambda^m \frac{\partial^m v_{gr}^{-1}(\lambda)}{\partial\lambda^m} \tag{65}$$

The inverse coefficients $\mathcal{K}(p,m)^{-1} = (-1)^{m-1} \frac{(p-2)!}{(m-1)!}$, $\mathcal{K}(p,0)^{-1} = 0$ are equivalent to the $\mathcal{E}(p-2, m-1)$ coefficients with shifted indices $m \le p-1$, as indicated in Table 7, Appendix E. Hence, using LLOF, a refined linear and nonlinear refractive index or an optical path function can be extracted from knowledge of the dispersion derivatives at a single point. Further, the dispersion can be optimized in reverse by altering the properties of novel materials and optical systems.

Written for the group velocity, the slopes of the dispersion parameter are:

$$\text{D I.}\ \frac{\partial v_{gr}^{-1}(\lambda)}{\partial\lambda} = -\frac{1}{c}\lambda\frac{\partial^2 n(\lambda)}{\partial\lambda^2} \qquad \text{D II.}\ \frac{\partial^2 v_{gr}^{-1}(\lambda)}{\partial\lambda^2} = -\frac{1}{c}\left(\frac{\partial^2 n(\lambda)}{\partial\lambda^2} + \lambda\frac{\partial^3 n(\lambda)}{\partial\lambda^3}\right) \tag{66}$$

$$\text{D III.}\ \frac{\partial^3 v_{gr}^{-1}(\lambda)}{\partial\lambda^3} = -\frac{1}{c}\left(2\frac{\partial^3 n(\lambda)}{\partial\lambda^3} + \lambda\frac{\partial^4 n(\lambda)}{\partial\lambda^4}\right) \qquad \text{D IV.}\ \frac{\partial^4 v_{gr}^{-1}(\lambda)}{\partial\lambda^4} = -\frac{1}{c}\left(3\frac{\partial^4 n(\lambda)}{\partial\lambda^4} + \lambda\frac{\partial^5 n(\lambda)}{\partial\lambda^5}\right) \tag{67}$$

$$\text{D V.}\ \frac{\partial^5 v_{gr}^{-1}(\lambda)}{\partial\lambda^5} = -\frac{1}{c}\left(4\frac{\partial^5 n(\lambda)}{\partial\lambda^5} + \lambda\frac{\partial^6 n(\lambda)}{\partial\lambda^6}\right) \qquad \text{D VI.}\ \frac{\partial^6 v_{gr}^{-1}(\lambda)}{\partial\lambda^6} = -\frac{1}{c}\left(5\frac{\partial^6 n(\lambda)}{\partial\lambda^6} + \lambda\frac{\partial^7 n(\lambda)}{\partial\lambda^7}\right) \tag{68}$$

$$\text{D VII.}\ \frac{\partial^7 v_{gr}^{-1}(\lambda)}{\partial\lambda^7} = -\frac{1}{c}\left(6\frac{\partial^7 n(\lambda)}{\partial\lambda^7} + \lambda\frac{\partial^8 n(\lambda)}{\partial\lambda^8}\right) \qquad \text{D VIII.}\ \frac{\partial^8 v_{gr}^{-1}(\lambda)}{\partial\lambda^8} = -\frac{1}{c}\left(7\frac{\partial^8 n(\lambda)}{\partial\lambda^8} + \lambda\frac{\partial^9 n(\lambda)}{\partial\lambda^9}\right) \tag{69}$$

$$\text{D IX.}\ \frac{\partial^9 v_{gr}^{-1}(\lambda)}{\partial\lambda^9} = -\frac{1}{c}\left(8\frac{\partial^9 n(\lambda)}{\partial\lambda^9} + \lambda\frac{\partial^{10} n(\lambda)}{\partial\lambda^{10}}\right) \qquad \text{D X.}\ \frac{\partial^{10} v_{gr}^{-1}(\lambda)}{\partial\lambda^{10}} = -\frac{1}{c}\left(9\frac{\partial^{10} n(\lambda)}{\partial\lambda^{10}} + \lambda\frac{\partial^{11} n(\lambda)}{\partial\lambda^{11}}\right) \tag{70}$$

Appendix E. Wavevector derivatives with respect to the wavelength and dispersion formulation in the wavelength space

When the dispersion is formulated in the wavelength space, as in Eqs. (26) and (27), the dispersion orders according to Eq. (28), representing the Lah-Laguerre transform for $\alpha = 0$, can be articulated as:

$$\frac{\partial^p}{\partial\lambda^p}\left(\frac{2\pi}{\lambda} f(\lambda)\right) = (-1)^p 2\pi \left(\frac{\omega}{2\pi c}\right)^{p+1} \sum_{m=0}^{p} \mathcal{D}(p,m)\, \omega^m \frac{\partial^m}{\partial\omega^m} f(\omega) \tag{71}$$

The inverse transform connects the Taylor coefficients of the refractive index or the optical path to the phase:

$$\omega^p \frac{\partial^p}{\partial\omega^p} f(\omega) = (-1)^p \frac{\lambda}{2\pi} \sum_{m=0}^{p} \mathcal{D}(p,m) \lambda^m \frac{\partial^m}{\partial\lambda^m}\left(\frac{2\pi}{\lambda} f(\lambda)\right) \tag{72}$$

Here, f is either the refractive index n or the optical path OP ($k(\lambda) = \frac{2\pi}{\lambda} n(\lambda)$ and $\varphi(\lambda) = \frac{2\pi}{\lambda} OP(\lambda)$). The corresponding matrix elements $\mathcal{D}(p,m) = \frac{p!}{(p-m)!m!}\frac{p!}{m!}$ are given in Table 5.

Optics EXPRESS

The expressions, written for the wavevector, are:

$$\text{E I.}\ \frac{\partial k(\lambda)}{\partial \lambda} = -2\pi\left(\frac{\omega}{2\pi c}\right)^2 G_1^{(0)}(\omega) = -2\pi\left(\frac{\omega}{2\pi c}\right)^2 \left(n(\omega) + \omega\frac{\partial n(\omega)}{\partial \omega}\right) \tag{73}$$

$$\text{E II.}\ \frac{\partial^2 k(\lambda)}{\partial \lambda^2} = 2\pi\left(\frac{\omega}{2\pi c}\right)^3 G_2^{(0)}(\omega) = 2\pi\left(\frac{\omega}{2\pi c}\right)^3 \left(2n(\omega) + 4\omega\frac{\partial n(\omega)}{\partial n\omega} + \omega^2\frac{\partial^2 n(\omega)}{\partial \omega^2}\right) \tag{74}$$

$$\text{E III.}\ \frac{\partial^3 k(\lambda)}{\partial \lambda^3} = -2\pi\left(\frac{\omega}{2\pi c}\right)^4 G_3^{(0)}(\omega) = -2\pi\left(\frac{\omega}{2\pi c}\right)^4 \left(6n(\omega) + 18\omega\frac{\partial n(\omega)}{\partial \omega} + 9\omega^2\frac{\partial^2 n(\omega)}{\partial \omega^2} + \right. \\ \left. + \omega^3\frac{\partial^3 n(\omega)}{\partial \omega^3}\right) \tag{75}$$

$$\text{E IV.}\ \frac{\partial^4 k(\lambda)}{\partial \lambda^4} = 2\pi\left(\frac{\omega}{2\pi c}\right)^5 G_4^{(0)}(\omega) = 2\pi\left(\frac{\omega}{2\pi c}\right)^5 \left(24n(\omega) + 96\omega\frac{\partial n(\omega)}{\partial \omega} + 72\omega^2\frac{\partial^2 n(\omega)}{\partial \omega^2} + \right. \\ \left. + 16\omega^3\frac{\partial^3 n(\omega)}{\partial \omega^3} + \omega^4\frac{\partial^4 n(\omega)}{\partial \omega^4}\right) \tag{76}$$

$$\text{E V.}\ \frac{\partial^5 k(\lambda)}{\partial \lambda^5} = -2\pi\left(\frac{\omega}{2\pi c}\right)^6 G_5^{(0)}(\omega) = -2\pi\left(\frac{\omega}{2\pi c}\right)^6 \left(120n(\omega) + 600\omega\frac{\partial n(\omega)}{\partial \omega} + \right. \\ \left. + 600\omega^2\frac{\partial^2 n(\omega)}{\partial \omega^2} + 200\omega^3\frac{\partial^3 n(\omega)}{\partial \omega^3} + 25\omega^4\frac{\partial^4 n(\omega)}{\partial \omega^4} + \omega^5\frac{\partial^5 n(\omega)}{\partial \omega^5}\right) \tag{77}$$

$$\text{E VI.}\ \frac{\partial^6 k(\lambda)}{\partial \lambda^6} = 2\pi\left(\frac{\omega}{2\pi c}\right)^7 G_6^{(0)}(\omega) = 2\pi\left(\frac{\omega}{2\pi c}\right)^7 \left(720n(\omega) + 4320\omega\frac{\partial n(\omega)}{\partial \omega} + \right. \\ \left. + 5400\omega^2\frac{\partial^2 n(\omega)}{\partial \omega^2} + 2400\omega^3\frac{\partial^3 n(\omega)}{\partial \omega^3} + 450\omega^4\frac{\partial^4 n(\omega)}{\partial \omega^4} + 36\omega^5\frac{\partial^5 n(\omega)}{\partial \omega^5} + \omega^6\frac{\partial^6 n(\omega)}{\partial \omega^6}\right) \tag{78}$$

$$\text{E VII.}\ \frac{\partial^7 k(\lambda)}{\partial \lambda^7} = -2\pi\left(\frac{\omega}{2\pi c}\right)^8 G_7^{(0)}(\omega) = -2\pi\left(\frac{\omega}{2\pi c}\right)^8 \left(5040n(\omega) + 35280\omega\frac{\partial n(\omega)}{\partial \omega} + \right. \\ \left. + 52920\omega^2\frac{\partial^2 n(\omega)}{\partial \omega^2} + 29400\omega^3\frac{\partial^3 n(\omega)}{\partial \omega^3} + 7350\omega^4\frac{\partial^4 n(\omega)}{\partial \omega^4} + 882\omega^5\frac{\partial^5 n(\omega)}{\partial \omega^5} + \right. \\ \left. + 49\omega^6\frac{\partial^6 n(\omega)}{\partial \omega^6} + \omega^7\frac{\partial^7 n(\omega)}{\partial \omega^7}\right) \tag{79}$$

$$\text{E VIII.}\ \frac{\partial^8 k(\lambda)}{\partial \lambda^8} = 2\pi\left(\frac{\omega}{2\pi c}\right)^9 G_8^{(0)}(\omega) = 2\pi\left(\frac{\omega}{2\pi c}\right)^9 \left(40320n(\omega) + 322560\omega\frac{\partial n(\omega)}{\partial \omega} + \right. \\ \left. + 564480\omega^2\frac{\partial^2 n(\omega)}{\partial \omega^2} + 376320\omega^3\frac{\partial^3 n(\omega)}{\partial \omega^3} + 117600\omega^4\frac{\partial^4 n(\omega)}{\partial \omega^4} + 18816\omega^5\frac{\partial^5 n(\omega)}{\partial \omega^5} + \right. \\ \left. + 1568\omega^6\frac{\partial^6 n(\omega)}{\partial \omega^6} + 64\omega^7\frac{\partial^7 n(\omega)}{\partial \omega^7} + \omega^8\frac{\partial^8 n(\omega)}{\partial \omega^8}\right) \tag{80}$$

$$\text{E IX.}\ \frac{\partial^9 k(\lambda)}{\partial \lambda^9} = -2\pi\left(\frac{\omega}{2\pi c}\right)^{10} G_9^{(0)}(\omega) = -2\pi\left(\frac{\omega}{2\pi c}\right)^{10} \left(362880n(\omega) + 3265920\omega\frac{\partial n(\omega)}{\partial \omega} + \right. \\ \left. + 6531840\omega^2\frac{\partial^2 n(\omega)}{\partial \omega^2} + 5080320\omega^3\frac{\partial^3 n(\omega)}{\partial \omega^3} + 1905120\omega^4\frac{\partial^4 n(\omega)}{\partial \omega^4} + 381024\omega^5\frac{\partial^5 n(\omega)}{\partial \omega^5} + \right. \\ \left. + 42336\omega^6\frac{\partial^6 n(\omega)}{\partial \omega^6} + 2592\omega^7\frac{\partial^7 n(\omega)}{\partial \omega^7} + 81\omega^8\frac{\partial^8 n(\omega)}{\partial \omega^8} + \omega^9\frac{\partial^9 n(\omega)}{\partial \omega^9}\right) \tag{81}$$

Optics EXPRESS

$$\text{E X.}\ \frac{\partial^{10}k(\lambda)}{\partial\lambda^{10}} = 2\pi\left(\frac{\omega}{2\pi c}\right)^{11} G_{10}^{(0)}(\omega) = 2\pi\left(\frac{\omega}{2\pi c}\right)^{11}\left(3628800n(\omega) + 36288000\omega\frac{\partial n(\omega)}{\partial\omega} + \right.$$
$$+ 81648000\omega^2\frac{\partial^2 n(\omega)}{\partial\omega^2} + 72576000\omega^3\frac{\partial^3 n(\omega)}{\partial\omega^3} + 31752000\omega^4\frac{\partial^4 n(\omega)}{\partial\omega^4} + 7620480\omega^5\frac{\partial^5 n(\omega)}{\partial\omega^5} + \tag{82}$$
$$\left. + \ 1058400\omega^6\frac{\partial^6 n(\omega)}{\partial\omega^6} + 86400\omega^7\frac{\partial^7 n(\omega)}{\partial\omega^7} + 4050\omega^8\frac{\partial^8 n(\omega)}{\partial\omega^8} + 100\omega^9\frac{\partial^9 n(\omega)}{\partial\omega^9} + \omega^{10}\frac{\partial^{10} n(\omega)}{\partial\omega^{10}}\right)$$

Table 5. Matrix elements $\mathcal{D}(p, m)$ up to the tenth order and unsigned Laguerre coefficients for $\alpha = 0$.

Dispersion order p		$d_\omega^{(0)}$ $m=0$	$d_\omega^{(1)}$ $m=1$	$d_\omega^{(2)}$ $m=2$	$d_\omega^{(3)}$ $m=3$	$d_\omega^{(4)}$ $m=4$	$d_\omega^{(5)}$ $m=5$	$d_\omega^{(6)}$ $m=6$	$d_\omega^{(7)}$ $m=7$	$d_\omega^{(8)}$ $m=8$	$d_\omega^{(9)}$ $m=9$	$d_\omega^{(10)}$ $m=10$
Zero	$p=0$	1	0	0	0	0	0	0	0	0	0	0
First	$p=1$	1	1	0	0	0	0	0	0	0	0	0
Second	$p=2$	2	4	1	0	0	0	0	0	0	0	0
Third	$p=3$	6	18	9	1	0	0	0	0	0	0	0
Fourth	$p=4$	24	96	72	16	1	0	0	0	0	0	0
Fifth	$p=5$	120	600	600	200	25	1	0	0	0	0	0
Sixth	$p=6$	720	4320	5400	2400	450	36	1	0	0	0	0
Seventh	$p=7$	5040	35280	52920	29400	7350	882	49	1	0	0	0
Eight	$p=8$	40320	322560	564480	376320	117600	18816	1568	64	1	0	0
Ninth	$p=9$	362880	3265920	6531840	5080320	1905120	381024	42336	2592	81	1	0
Tenth	p=10	3628800	36288000	81648000	72576000	31752000	7620480	1058400	86400	4050	100	1

The derivatives of $k(\lambda) = \frac{2\pi}{\lambda}n(\lambda)$ and $\varphi(\lambda) = \frac{2\pi}{\lambda}OP(\lambda)$ in terms of the wavelength can be obtained through the transform specified in Eq. (29):

$$\frac{\partial^p}{\partial\lambda^p}\left(\frac{2\pi}{\lambda}f(\lambda)\right) = (-1)^p 2\pi\lambda^{-(p+1)}\sum_{m=0}^{p}\mathcal{E}(p,m)\lambda^m\frac{\partial^m}{\partial\lambda^m}f(\lambda) \tag{83}$$

The inverse transform connects the Taylor coefficients of the refractive index or the optical path to the phase, in the most convenient computational form:

$$\frac{\partial^p}{\partial\lambda^p}f(\lambda) = \frac{\lambda^{1-p}}{2\pi}\sum_{m=0}^{p}\mathcal{V}(p,m)\lambda^m\frac{\partial^m}{\partial\lambda^m}\left(\frac{2\pi}{\lambda}f(\lambda)\right) =$$
$$= \frac{1}{2\pi}\left(p\frac{\partial^{p-1}}{\partial\lambda^{p-1}}\left(\frac{2\pi}{\lambda}f(\lambda)\right) + \lambda\frac{\partial^p}{\partial\lambda^p}\left(\frac{2\pi}{\lambda}f(\lambda)\right)\right) \tag{84}$$

Here, knowledge of the phase derivatives at a single point reproduces the refractive index (linear and nonlinear) in an extended vicinity of the considered point through the calculated Taylor coefficients of the refractive index, enabling more precise refractive index measurements and optimization of the dispersion in reverse.

The refractive index $n(\lambda)$, and optical path $OP(\lambda)$ are interchangeable in Eq. (29) for the derivatives of $k(\lambda) = \frac{2\pi}{\lambda}n(\lambda)$ and $\varphi(\lambda) = \frac{2\pi}{\lambda}OP(\lambda)$. The corresponding matrix elements $\mathcal{E}(p,m) = (-1)^m\frac{p!}{m!}$ are listed in Table 6.

Optics EXPRESS

Table 6. Matrix elements $\mathcal{E}(p, m)$ up to the tenth order.

Dispersion order p		$d_\lambda^{(0)}$ $m=0$	$d_\lambda^{(1)}$ $m=1$	$d_\lambda^{(2)}$ $m=2$	$d_\lambda^{(3)}$ $m=3$	$d_\lambda^{(4)}$ $m=4$	$d_\lambda^{(5)}$ $m=5$	$d_\lambda^{(6)}$ $m=6$	$d_\lambda^{(7)}$ $m=7$	$d_\lambda^{(8)}$ $m=8$	$d_\lambda^{(9)}$ $m=9$	$d_\lambda^{(10)}$ $m=10$
Zero	$p=0$	1	0	0	0	0	0	0	0	0	0	0
First	$p=1$	1	−1	0	0	0	0	0	0	0	0	0
Second	$p=2$	2	−2	1	0	0	0	0	0	0	0	0
Third	$p=3$	6	−6	3	−1	0	0	0	0	0	0	0
Fourth	$p=4$	24	−24	12	−4	1	0	0	0	0	0	0
Fifth	$p=5$	120	−120	60	−20	5	−1	0	0	0	0	0
Sixth	$p=6$	720	−720	360	−120	30	−6	1	0	0	0	0
Seventh	$p=7$	5040	−5040	2520	−840	210	−42	7	−1	0	0	0
Eight	$p=8$	40320	−40320	20160	−6720	1680	−336	56	−8	1	0	0
Ninth	$p=9$	362880	−362880	181440	−60480	15120	−3024	504	−72	9	−1	0
Tenth	$p=10$	3628800	−3628800	1814400	−604800	151200	−30240	5040	−720	90	−10	1

The expressions, written for the wavevector, are :

$$\text{EE I.}\ \frac{\partial k(\lambda)}{\partial \lambda} = -2\pi\lambda^{-2}\left(n(\lambda) - \lambda\frac{\partial n(\lambda)}{\partial \lambda}\right) \tag{85}$$

$$\text{EE II.}\ \frac{\partial^2 k(\lambda)}{\partial \lambda^2} = \frac{\partial}{\partial \lambda}\left(\frac{\partial k(\lambda)}{\partial \lambda}\right) = 2\pi\lambda^{-3}\left(2n(\lambda) - 2\lambda\frac{\partial n(\lambda)}{\partial \lambda} + \lambda^2\frac{\partial^2 n(\lambda)}{\partial \lambda^2}\right) \tag{86}$$

$$\text{EE III.}\ \frac{\partial^3 k(\lambda)}{\partial \lambda^3} = -2\pi\lambda^{-4}\left(6n(\lambda) - 6\lambda\frac{\partial n(\lambda)}{\partial \lambda} + 3\lambda^2\frac{\partial^2 n(\lambda)}{\partial \lambda^2} - \lambda^3\frac{\partial^3 n(\lambda)}{\partial \lambda^3}\right) \tag{87}$$

$$\text{EE IV.}\ \frac{\partial^4 k(\lambda)}{\partial \lambda^4} = 2\pi\lambda^{-5}\left(24n(\lambda) - 24\lambda\frac{\partial n(\lambda)}{\partial \lambda} + 12\lambda^2\frac{\partial^2 n(\lambda)}{\partial \lambda^2} - 4\lambda^3\frac{\partial^3 n(\lambda)}{\partial \lambda^3} + \lambda^4\frac{\partial^4 n(\lambda)}{\partial \lambda^4}\right) \tag{88}$$

$$\text{EE V.}\ \frac{\partial^5 n(\lambda)}{\partial \lambda^5} = -2\pi\lambda^{-6}\left(120n(\lambda) - 120\lambda\frac{\partial n(\lambda)}{\partial \lambda} + 60\lambda^2\frac{\partial^2 n(\lambda)}{\partial \lambda^2} - 20\lambda^3\frac{\partial^3 n(\lambda)}{\partial \lambda^3} + 5\lambda^4\frac{\partial^4 n(\lambda)}{\partial \lambda^4} + - \lambda^5\frac{\partial^5 n(\lambda)}{\partial \lambda^5}\right) \tag{89}$$

$$\text{EE VI.}\ \frac{\partial^6 k(\lambda)}{\partial \lambda^6} = 2\pi\lambda^{-7}\left(720n(\lambda) - 720\lambda\frac{\partial n(\lambda)}{\partial \lambda} + 360\lambda^2\frac{\partial^2 n(\lambda)}{\partial \lambda^2} - 120\lambda^3\frac{\partial^3 n(\lambda)}{\partial \lambda^3} + + 30\lambda^4\frac{\partial^4 n(\lambda)}{\partial \lambda^4} - 6\lambda^5\frac{\partial^5 n(\lambda)}{\partial \lambda^5} + \lambda^6\frac{\partial^6 n(\lambda)}{\partial \lambda^6}\right) \tag{90}$$

$$\text{EE VII.}\ \frac{\partial^7 k(\lambda)}{\partial \lambda^7} = -2\pi\lambda^{-8}\left(5040n(\lambda) - 5040\lambda\frac{\partial n(\lambda)}{\partial \lambda} + 2520\lambda^2\frac{\partial^2 n(\lambda)}{\partial \lambda^2} - 840\lambda^3\frac{\partial^3 n(\lambda)}{\partial \lambda^3} + + 210\lambda^4\frac{\partial^4 n(\lambda)}{\partial \lambda^4} - 42\lambda^5\frac{\partial^5 n(\lambda)}{\partial \lambda^5} + 7\lambda^6\frac{\partial^6 n(\lambda)}{\partial \lambda^6} - \lambda^7\frac{\partial^7 n(\lambda)}{\partial \lambda^7}\right) \tag{91}$$

$$\text{EE VIII.}\ \frac{\partial^8 k(\lambda)}{\partial \lambda^8} = 2\pi\lambda^{-9}\left(40320n(\lambda) - 40320\lambda\frac{\partial n(\lambda)}{\partial \lambda} + 20160\lambda^2\frac{\partial^2 n(\lambda)}{\partial \lambda^2} - 6720\lambda^3\frac{\partial^3 n(\lambda)}{\partial \lambda^3} + + 1680\lambda^4\frac{\partial^4 n(\lambda)}{\partial \lambda^4} - 336\lambda^5\frac{\partial^5 n(\lambda)}{\partial \lambda^5} + 56\lambda^6\frac{\partial^6 n(\lambda)}{\partial \lambda^6} - 8\lambda^7\frac{\partial^7 n(\lambda)}{\partial \lambda^7} + \lambda^8\frac{\partial^8 n(\lambda)}{\partial \lambda^8}\right) \tag{92}$$

Optics EXPRESS

$$\text{EE IX. } \frac{\partial^9 k(\lambda)}{\partial\lambda^9} = -2\pi\lambda^{-10}\Big(362880n(\lambda) - 362880\lambda\frac{\partial n(\lambda)}{\partial\lambda} + 181440\lambda^2\frac{\partial^2 n(\lambda)}{\partial\lambda^2} + \\ - 60480\lambda^3\frac{\partial^3 n(\lambda)}{\partial\lambda^3} + 15120\lambda^4\frac{\partial^4 n(\lambda)}{\partial\lambda^4} - 3024\lambda^5\frac{\partial^5 n(\lambda)}{\partial\lambda^5} + 504\lambda^6\frac{\partial^6 n(\lambda)}{\partial\lambda^6} - 72\lambda^7\frac{\partial^7 n(\lambda)}{\partial\lambda^7} + \\ + 9\lambda^8\frac{\partial^8 n(\lambda)}{\partial\lambda^8} - \lambda^9\frac{\partial^9 n(\lambda)}{\partial\lambda^9}\Big) \tag{93}$$

$$\text{EE X. } \frac{\partial^{10} k(\lambda)}{\partial\lambda^{10}} = 2\pi\lambda^{-11}\Big(3628800n(\lambda) - 3628800\lambda\frac{\partial n(\lambda)}{\partial\lambda} + 1814400\lambda^2\frac{\partial^2 n(\lambda)}{\partial\lambda^2} + \\ - 604800\lambda^3\frac{\partial^3 n(\lambda)}{\partial\lambda^3} + 151200\lambda^4\frac{\partial^4 n(\lambda)}{\partial\lambda^4} - 30240\lambda^5\frac{\partial^5 n(\lambda)}{\partial\lambda^5} + 5040\lambda^6\frac{\partial^6 n(\lambda)}{\partial\lambda^6} - 720\lambda^7\frac{\partial^7 n(\lambda)}{\partial\lambda^7} + \\ + 90\lambda^8\frac{\partial^8 n(\lambda)}{\partial\lambda^8} - 10\lambda^9\frac{\partial^9 n(\lambda)}{\partial\lambda^9} + \lambda^{10}\frac{\partial^{10} n(\lambda)}{\partial\lambda^{10}}\Big) \tag{94}$$

Referring to Eq. (65), Appendix D, the inverse coefficients $\mathcal{K}(p,m)^{-1} = (-1)^{m-1}\frac{(p-2)!}{(m-1)!}$, $\mathcal{K}(p,0)^{-1} = 0$ are equivalent to the $\mathcal{E}(p-2,m-1)$ coefficients with shifted indices, $m \le p-1$. The corresponding coefficients are listed in Table 7.

Table 7. Matrix elements $\mathcal{K}(p,m)^{-1}$ and $\mathcal{E}(p-2,m-1)$ up to the eleventh order.

Dispersion order p		$d_\lambda^{(1)}$ $m=1$	$d_\lambda^{(2)}$ $m=2$	$d_\lambda^{(3)}$ $m=3$	$d_\lambda^{(4)}$ $m=4$	$d_\lambda^{(5)}$ $m=5$	$d_\lambda^{(6)}$ $m=6$	$d_\lambda^{(7)}$ $m=7$	$d_\lambda^{(8)}$ $m=8$	$d_\lambda^{(9)}$ $m=9$	$d_\lambda^{(10)}$ $m=10$
Second	$p=2$	1	0	0	0	0	0	0	0	0	0
Third	$p=3$	1	−1	0	0	0	0	0	0	0	0
Fourth	$p=4$	2	−2	1	0	0	0	0	0	0	0
Fifth	$p=5$	6	−6	3	−1	0	0	0	0	0	0
Sixth	$p=6$	24	−24	12	−4	1	0	0	0	0	0
Seventh	$p=7$	120	−120	60	−20	5	−1	0	0	0	0
Eight	$p=8$	720	−720	360	−120	30	−6	1	0	0	0
Ninth	$p=9$	5040	−5040	2520	−840	210	−42	7	−1	0	0
Tenth	$p=10$	40320	−40320	20160	−6720	1680	−336	56	−8	1	0
Eleventh	$p=11$	362880	−362880	181440	−60480	15120	−3024	504	−72	9	−1

The expressions, written for the refractive index $n(\lambda)$, are:

$$\lambda^p\frac{\partial^p}{\partial\lambda^p}n(\lambda) = (-1)^{p+1}c\sum_{m=0}^{p-1}\mathcal{K}(p,m)^{-1}\lambda^m\frac{\partial^m}{\partial\lambda^m}v_{gr}^{-1}(\lambda) \tag{95}$$

$$\text{EEE I. } n(\lambda) - \lambda\frac{\partial n(\lambda)}{\partial\lambda} = cv_{gr}^{-1}(\lambda) \tag{96}$$

$$\text{EEE II. } \frac{\partial^2 n(\lambda)}{\partial\lambda^2} = -c\lambda^{-2}\Big(\lambda\frac{\partial v_{gr}^{-1}(\lambda)}{\partial\lambda}\Big) \tag{97}$$

$$\text{EEE III. } \frac{\partial^3 n(\lambda)}{\partial\lambda^3} = c\lambda^{-3}\Big(\lambda\frac{\partial v_{gr}^{-1}(\lambda)}{\partial\lambda} - \lambda^2\frac{\partial^2 v_{gr}^{-1}(\lambda)}{\partial\lambda^2}\Big) \tag{98}$$

$$\text{EEE IV. } \frac{\partial^4 n(\lambda)}{\partial\lambda^4} = -c\lambda^{-4}\Big(2\lambda\frac{\partial v_{gr}^{-1}(\lambda)}{\partial\lambda} - 2\lambda^2\frac{\partial^2 v_{gr}^{-1}(\lambda)}{\partial\lambda^2} + \lambda^3\frac{\partial^3 v_{gr}^{-1}(\lambda)}{\partial\lambda^3}\Big) \tag{99}$$

Optics EXPRESS

$$\text{EEE V. } \frac{\partial^5 n(\lambda)}{\partial\lambda^5} = c\lambda^{-5}\left(6\lambda\frac{\partial v_{gr}^{-1}(\lambda)}{\partial\lambda} - 6\lambda^2\frac{\partial^2 v_{gr}^{-1}(\lambda)}{\partial\lambda^2} + 3\lambda^3\frac{\partial^3 v_{gr}^{-1}(\lambda)}{\partial\lambda^3} - \lambda^4\frac{\partial^4 v_{gr}^{-1}(\lambda)}{\partial\lambda^4}\right) \tag{100}$$

$$\text{EEE VI. } \frac{\partial^6 n(\lambda)}{\partial\lambda^6} = -c\lambda^{-6}\left(24\lambda\frac{\partial v_{gr}^{-1}(\lambda)}{\partial\lambda} - 24\lambda^2\frac{\partial^2 v_{gr}^{-1}(\lambda)}{\partial\lambda^2} + 12\lambda^3\frac{\partial^3 v_{gr}^{-1}(\lambda)}{\partial\lambda^3} - 4\lambda^4\frac{\partial^4 v_{gr}^{-1}(\lambda)}{\partial\lambda^4} + \right. \tag{101}$$
$$\left. + \lambda^5\frac{\partial^5 v_{gr}^{-1}(\lambda)}{\partial\lambda^5}\right)$$

$$\text{EEE VII. } \frac{\partial^7 n(\lambda)}{\partial\lambda^7} = c\lambda^{-7}\left(120\lambda\frac{\partial v_{gr}^{-1}(\lambda)}{\partial\lambda} - 120\lambda^2\frac{\partial^2 v_{gr}^{-1}(\lambda)}{\partial\lambda^2} + 60\lambda^3\frac{\partial^3 v_{gr}^{-1}(\lambda)}{\partial\lambda^3} - 20\lambda^4\frac{\partial^4 v_{gr}^{-1}(\lambda)}{\partial\lambda^4} + \right. \tag{102}$$
$$\left. + 5\lambda^5\frac{\partial^5 v_{gr}^{-1}(\lambda)}{\partial\lambda^5} - \lambda^6\frac{\partial^6 v_{gr}^{-1}(\lambda)}{\partial\lambda^6}\right)$$

$$\text{EEE VIII. } \frac{\partial^8 n(\lambda)}{\partial\lambda^8} = -c\lambda^{-8}\left(720\lambda\frac{\partial v_{gr}^{-1}(\lambda)}{\partial\lambda} - 720\lambda^2\frac{\partial^2 v_{gr}^{-1}(\lambda)}{\partial\lambda^2} + 360\lambda^3\frac{\partial^3 v_{gr}^{-1}(\lambda)}{\partial\lambda^3} - 120\lambda^4\frac{\partial^4 v_{gr}^{-1}(\lambda)}{\partial\lambda^4} + \right. \tag{103}$$
$$\left. + 30\lambda^5\frac{\partial^5 v_{gr}^{-1}(\lambda)}{\partial\lambda^5} - 6\lambda^6\frac{\partial^6 v_{gr}^{-1}(\lambda)}{\partial\lambda^6} + \lambda^7\frac{\partial^7 v_{gr}^{-1}(\lambda)}{\partial\lambda^7}\right)$$

$$\text{EEE IX. } \frac{\partial^9 n(\lambda)}{\partial\lambda^9} = c\lambda^{-9}\left(5040\lambda\frac{\partial v_{gr}^{-1}(\lambda)}{\partial\lambda} - 5040\lambda^2\frac{\partial^2 v_{gr}^{-1}(\lambda)}{\partial\lambda^2} + 2520\lambda^3\frac{\partial^3 v_{gr}^{-1}(\lambda)}{\partial\lambda^3} - 840\lambda^4\frac{\partial^4 v_{gr}^{-1}(\lambda)}{\partial\lambda^4} + \right. \tag{104}$$
$$\left. + 210\lambda^5\frac{\partial^5 v_{gr}^{-1}(\lambda)}{\partial\lambda^5} - 42\lambda^6\frac{\partial^6 v_{gr}^{-1}(\lambda)}{\partial\lambda^6} + 7\lambda^7\frac{\partial^7 v_{gr}^{-1}(\lambda)}{\partial\lambda^7} - \lambda^8\frac{\partial^8 v_{gr}^{-1}(\lambda)}{\partial\lambda^8}\right)$$

$$\text{EEE X. } \frac{\partial^{10} n(\lambda)}{\partial\lambda^{10}} = -c\lambda^{-10}\left(40320\lambda\frac{\partial v_{gr}^{-1}(\lambda)}{\partial\lambda} - 40320\lambda^2\frac{\partial^2 v_{gr}^{-1}(\lambda)}{\partial\lambda^2} + 20160\lambda^3\frac{\partial^3 v_{gr}^{-1}(\lambda)}{\partial\lambda^3} + \right.$$
$$- 6720\lambda^4\frac{\partial^4 v_{gr}^{-1}(\lambda)}{\partial\lambda^4} + 1680\lambda^5\frac{\partial^5 v_{gr}^{-1}(\lambda)}{\partial\lambda^5} - 336\lambda^6\frac{\partial^6 v_{gr}^{-1}(\lambda)}{\partial\lambda^6} + 56\lambda^7\frac{\partial^7 v_{gr}^{-1}(\lambda)}{\partial\lambda^7} - 8\lambda^8\frac{\partial^8 v_{gr}^{-1}(\lambda)}{\partial\lambda^8} + \tag{105}$$
$$\left. + \lambda^9\frac{\partial^9 v_{gr}^{-1}(\lambda)}{\partial\lambda^9}\right)$$

Here $c = 299\,792\,458\ m/s$ is the speed of light in vacuum.

Appendix F. Identities

$$\text{F I. } x^p = \sum\nolimits_{m=0}^{p}\sum_{k=0}^{m}(-1)^{p-m}\mathcal{A}(p,m)\mathcal{A}(m,k)x^k \tag{106}$$

$$\text{F II. } x^p = \sum_{m=0}^{p}\sum_{k=0}^{m}(-1)^{p-m}\mathcal{B}(p,m)\mathcal{B}(m,k)\,x^k \tag{107}$$

$$\text{F III. } x^p = \sum_{m=0}^{p}\sum_{k=0}^{m}(-1)^{p-m}C(p,m)C(m,k)x^k \tag{108}$$

$$\text{F IV. } x^p = \sum_{m=0}^{p}\sum_{k=0}^{m}(-1)^{p-m}\mathcal{D}(p,m)\mathcal{D}(m,k)x^k \tag{109}$$

$$\text{F V. } x^p = \sum_{m=0}^{p}\sum_{k=0}^{m}(-1)^{m}\mathcal{V}(p,m)\mathcal{E}(m,k)x^k \tag{110}$$

$$\text{F VI. } u^p = (-1)^p\sum_{m=0}^{p}\sum_{k=0}^{m}\mathcal{V}(p,m)\mathcal{E}(m,k)u^k \tag{111}$$

Optics EXPRESS

$$\text{F VII. } x^p = \sum_{m=2}^{p+1}\sum_{k=1}^{m-1}(-1)^{m+1}\mathcal{K}(p,m)\mathcal{E}(m-2,k-1)x^k \tag{112}$$

$$\text{F VIII. } u^p = (-1)^{p+1}\sum_{m=1}^{p-1}\sum_{k=0}^{m+1}\mathcal{E}(m-2,k-1)\mathcal{K}(p,m)u^k \tag{113}$$

$$\text{F IX. } \mathcal{D}(p,k) = \sum_{m=0}^{p}(-1)^m\mathcal{E}(p,m)\mathcal{A}(m,k) \tag{114}$$

$$\text{F X. } \mathcal{K}(p,k) = \sum_{m=0}^{p+1}(-1)^{p-m}\mathcal{A}(p,m)\mathcal{B}(m+1,k) \tag{115}$$

$$\text{F XI. } \mathcal{V}(p,k) = \sum_{m=0}^{p}(-1)^{p-m}\mathcal{B}(p,m)\mathcal{A}(m,k) \tag{116}$$

$$\text{F XII. } \frac{\partial^{p+k}}{\partial\omega^{p+k}}\varphi(\omega) = \frac{\partial^p}{\partial\omega^p}KOD = (-1)^p\left(\frac{\lambda}{2\pi c}\right)^p\sum_{m=0}^{p}\mathcal{A}(p,m)\,\lambda^m\frac{\partial^m}{\partial\lambda^m}KOD(\lambda) \tag{117}$$

where KOD is the k^{th} order of dispersion. The lower dispersion terms $n<k$ can be obtained simpler from the even dispersion terms (k even), with the help of the Cauchy formula:

$$\text{F XIII. } \frac{\partial^{k-n}}{\partial\omega^{k-n}}\varphi(\omega) = \int\ldots\int_{\omega_{zd}}^{\omega}KOD(\omega)d\omega\ldots d\omega = \int_{\omega_{zd}}^{\omega}KOD(t)\frac{(\omega-t)^{n-1}}{\Gamma(n)}dt \tag{118}$$

where ω_{zd} is the zero dispersion frequency of the KOD, and $\Gamma(n)$ is the gamma function.

Funding. H2020 European Research Council (XSTREAM-716950); Alfred P. Sloan Foundation (FG-2018-10892).

Acknowledgments. This study has received funding from the European Research Council (ERC) under the European Union's Horizon 2020 research and innovation program (grant agreement XSTREAM-716950). In addition, TP gratefully acknowledges the support of the Alfred P. Sloan Foundation (FG-2018-10892).

Disclosures. The authors declare no conflicts of interest.

Data availability. Data files and plots for the first ten orders of the material dispersion of CaF_2, sapphire, fused silica, *BK7*, *BBO* (for the ordinary and extraordinary axes), water, liquid *Ar*, and several gases at standard conditions (air, *He*, *Ne*, *Ar*, *Kr*, *Xe*, H_2, O_2, and N_2), obtained using the Lah-Laguerre optical formalism, are available in Dataset 1, Ref. [36].

References

1. N. Niizeki, "Single mode fiber at zero-dispersion wavelength," in *Topical Meeting on Integrated and Guided Wave Optics*, vol. 16 (1968).
2. C. DeCusatis, ed., *Handbook of Fiber Optic Data Communication* (Academic Press, , Oxford, 2013).
3. G. Agrawal, *Nonlinear Fiber Optics (Fifth Edition)* (Academic Press, Boston, 2013).
4. M. Carson, *Alexander Graham Bell: Giving Voice to the World* (Sterling, 2007).
5. S. Hemati and M. Emadi, "A method for analyzing higher-order dispersion in optical fiber," in *CCECE 2003 - Canadian Conference on Electrical and Computer Engineering. Toward a Caring and Humane Technology (Cat. No.03CH37436)*, vol. 1 (2003), pp. 289–292 vol.1.
6. International Telecommunication Union, "ITU standard G.655 (11/09), characteristics of a non-zero dispersion-shifted single-mode optical fibre and cable," (2009).
7. E. Hüttmann, "Distance measuring method (ranging method)," German Patent 768, 068 (1940).
8. C. E. Cook, "Pulse compression-key to more efficient radar transmission," Proc. IRE **48**(3), 310–316 (1960).
9. D. Strickland and G. Mourou, "Compression of amplified chirped optical pulses," Opt. Commun. **56**(3), 219–221 (1985).
10. E. Treacy, "Optical pulse compression with diffraction gratings," IEEE J. Quantum Electron. **5**(9), 454–458 (1969).
11. R. L. Fork, O. E. Martinez, and J. P. Gordon, "Negative dispersion using pairs of prisms," Opt. Lett. **9**(5), 150–152 (1984).
12. J. Heppner and J. Kuhl, "Intracavity chirp compensation in a colliding pulse mode-locked laser using thin-film interferometers," Appl. Phys. Lett. **47**(5), 453–455 (1985).

Optics EXPRESS

13. M. Yamashita, K. Torizuka, and T. Sato, "A chirp-compensation technique using incident-angle changes of cavity mirrors in a femtosecond pulse laser," IEEE J. Quantum Electron. **23**(11), 2005–2007 (1987).
14. R. Szipöcs, K. Ferencz, C. Spielmann, and F. Krausz, "Chirped multilayer coatings for broadband dispersion control in femtosecond lasers," Opt. Lett. **19**(3), 201–203 (1994).
15. J.-C. Diels and W. Rudolph, eds., *Ultrashort Laser Pulse Phenomena* (Academic Press, Burlington, 2006), 2nd ed.
16. P. A. Naik and A. K. Sharma, "Calculation of higher order group velocity dispersion in a grating pulse stretcher / compressor using recursion method," J. Opt. **29**(3), 105–113 (2000).
17. D. Popmintchev, C. Hernández-García, F. Dollar, C. Mancuso, J. A. Pérez-Hernández, M.-C. Chen, A. Hankla, X. Gao, B. Shim, A. L. Gaeta, M. Tarazkar, D. A. Romanov, R. J. Levis, J. A. Gaffney, M. Foord, S. B. Libby, A. Jaron-Becker, A. Becker, L. Plaja, M. M. Murnane, H. C. Kapteyn, and T. Popmintchev, "Ultraviolet surprise: Efficient soft X-ray high-harmonic generation in multiply ionized plasmas," Science **350**(6265), 1225–1231 (2015).
18. D. Popmintchev, B. R. Galloway, M.-C. Chen, F. Dollar, C. A. Mancuso, A. Hankla, L. Miaja-Avila, G. O'Neil, J. M. Shaw, G. Fan, S. Ališauskas, G. Andriukaitis, T. Balciunas, O. D. Mücke, A. Pugzlys, A. Baltuška, H. C. Kapteyn, T. Popmintchev, and M. M. Murnane, "Near- and extended-edge X-ray-absorption fine-structure spectroscopy using ultrafast coherent high-order harmonic supercontinua," Phys. Rev. Lett. **120**(9), 093002 (2018).
19. T. Popmintchev, M.-C. Chen, D. Popmintchev, P. Arpin, S. Brown, S. Ališauskas, G. Andriukaitis, T. Balciunas, O. D. Mücke, A. Pugzlys, A. Baltuška, B. Shim, S. E. Schrauth, A. Gaeta, C. Hernández-García, L. Plaja, A. Becker, A. Jaron-Becker, M. M. Murnane, and H. C. Kapteyn, "Bright coherent ultrahigh harmonics in the kev x-ray regime from mid-infrared femtosecond lasers," Science **336**(6086), 1287–1291 (2012).
20. P. S. J. Russell, P. Hölzer, W. Chang, A. Abdolvand, and J. C. Travers, "Hollow-core photonic crystal fibres for gas-based nonlinear optics," Nat. Photonics **8**(4), 278–286 (2014).
21. X. Ding, M. Selim Habib, R. Amezcua-Correa, and J. Moses, "Near-octave intense mid-infrared by adiabatic down-conversion in hollow anti-resonant fiber," Opt. Lett. **44**(5), 1084–1087 (2019).
22. A. I. Adamu, M. S. Habib, C. R. Petersen, J. E. A. Lopez, B. Zhou, A. Schülzgen, M. Bache, R. Amezcua-Correa, O. Bang, and C. Markos, "Deep-UV to mid-ir supercontinuum generation driven by mid-IR ultrashort pulses in a gas-filled hollow-core fiber," Sci. Rep. **9**(1), 4446 (2019).
23. J. Capmany, D. Pastor, S. Sales, and M. A. Muriel, "Pulse distortion in optical fibers and waveguides with arbitrary chromatic dispersion," J. Opt. Soc. Am. B **20**(12), 2523–2533 (2003).
24. M. Amemiya, "Pulse broadening due to higher order dispersion and its transmission limit," J. Lightwave Technol. **20**(4), 591–597 (2002).
25. I. Lah, "A new kind of numbers and its application in the actuarial mathematics," Boletim do Instituto dos Actuarios Portugueses **9**, 7–15 (1954).
26. J. Riordan, *Introduction to Combinatorial Analysis* (Dover Publications, 1958), 1st ed.
27. OEIS Foundation Inc., The On-Line Encyclopedia of Integer Sequences, http://oeis.org (2022).
28. G. Kilibarda and V. Jovovic, "Antichains of multisets," Journal of Integer Sequences **7** (2004).
29. P. Barry, "Some observations on the Lah and Laguerre transforms of integer sequences," Journal of Integer Sequences **10** (2007).
30. N. B. Khristo, "Lah numbers, laguerre polynomials of order negative one, and the nth derivative of exp (1/*x*)," Acta Universitatis Sapientiae, Mathematica **8**(1), 22–31 (2016).
31. R. W. Boyd, ed., *Nonlinear Optics* (Academic Press, 2020), 4th ed.
32. Refractive index database, https://refractiveindex.info (2022).
33. H. H. Li, "Refractive index of alkaline earth halides and its wavelength and temperature derivatives," J. Phys. Chem. Ref. Data **9**(1), 161–290 (1980).
34. J. H. Burnett, Z. H. Levine, and E. L. Shirley, "Intrinsic birefringence in calcium fluoride and barium fluoride," Phys. Rev. B **64**(24), 241102 (2001).
35. J. B. W. Webber, "A bi-symmetric log transformation for wide-range data," Meas. Sci. Technol. **24**(2), 027001 (2013).
36. D. Popmintchev, S. Wang, X. Zhang, V. Stoev, and T. Popmintchev, "Dispersion orders of various materials," figshare (2022), https://doi.org/10.6084/m9.figshare.19236792.
37. S. Backus, C. Durfee, M. Murnane, and H. Kapteyn, "High power ultrafast lasers," Rev. Sci. Instrum. **69**(3), 1207–1223 (1998).
38. W. E. White, F. G. Patterson, R. L. Combs, D. F. Price, and R. L. Shepherd, "Compensation of higher-order frequency-dependent phase terms in chirped-pulse amplification systems," Opt. Lett. **18**(16), 1343–1345 (1993).
39. S. Kane, J. Squier, J. V. Rudd, and G. Mourou, "Hybrid grating–prism stretcher–compressor system with cubic phase and wavelength tunability and decreased alignment sensitivity," Opt. Lett. **19**(22), 1876–1878 (1994).
40. S. Li, C. Wang, Y. Liu, Y. Xu, Y. Li, X. Liu, Z. Gan, L. Yu, X. Liang, Y. Leng, and R. Li, "High-order dispersion control of 10 Petawatt Ti:Sapphire laser facility," Opt. Express **25**(15), 17488–17498 (2017).
41. C. Wang, S. Li, Y. Liu, X. Liu, Y. Leng, and R. Li, "Hybrid grating–prism dispersion eraser," Opt. Commun. **411**, 88–92 (2018).
42. V. Stoev, K. Holsinger, D. S. Bell, and O. Korth, "Automated bandwidth/wavelength adjustment systems and methods for short pulse lasers and optical amplifiers," (2012). US Patent 8, 218, 587.
43. Q. Yang, X. Xie, J. Kang, H. Zhu, A. Guo, and Q. Gao, "Independent and continuous third-order dispersion compensation using a pair of prisms," High Power Laser Sci. Eng. **2**, e38 (2014).

Optics EXPRESS

44. W. Dietel, J. J. Fontaine, and J. C. Diels, "Intracavity pulse compression with glass: a new method of generating pulses shorter than 60 fs," Opt. Lett. **8**(1), 4–6 (1983).
45. A. D. Pryamikov, A. S. Biriukov, A. F. Kosolapov, V. G. Plotnichenko, S. L. Semjonov, and E. M. Dianov, "Demonstration of a waveguide regime for a silica hollow - core microstructured optical fiber with a negative curvature of the core boundary in the spectral region $> 3.5\ \mu m$," Opt. Express **19**(2), 1441–1448 (2011).
46. M. Zeisberger and M. A. Schmidt, "Analytic model for the complex effective index of the leaky modes of tube-type anti-resonant hollow core fibers," Sci. Rep. **7**(1), 11761 (2017).
47. J. Archambault, R. J. Black, S. Lacroix, and J. Bures, "Loss calculations for antiresonant waveguides," J. Lightwave Technol. **11**(3), 416–423 (1993).
48. A. Taranta, E. Numkam Fokoua, S. Abokhamis Mousavi, J. R. Hayes, T. D. Bradley, G. T. Jasion, and F. Poletti, "Exceptional polarization purity in antiresonant hollow-core optical fibres," Nat. Photonics **14**(8), 504–510 (2020).
49. I. H. Malitson, "Interspecimen comparison of the refractive index of fused silica," J. Opt. Soc. Am. **55**(10), 1205–1209 (1965).
50. C. Z. Tan, "Determination of refractive index of silica glass for infrared wavelengths by IR spectroscopy," J. Non-Cryst. Solids **223**(1-2), 158–163 (1998).
51. M. Daimon and A. Masumura, "High-accuracy measurements of the refractive index and its temperature coefficient of calcium fluoride in a wide wavelength range from 138 to 2326 nm," Appl. Opt. **41**(25), 5275–5281 (2002).
52. H. Sakr, T. D. Bradley, G. T. Jasion, E. N. Fokoua, S. R. Sandoghchi, I. A. Davidson, A. Taranta, G. Guerra, W. Shere, Y. Chen, J. R. Hayes, D. J. Richardson, and F. Poletti, "Hollow core NANFs with five nested tubes and record low loss at 850, 1060, 1300 and 1625nm," in *2021 Optical Fiber Communications Conference and Exhibition (OFC)*, (2021), pp. 1–3.